Case Studies in Construction Materials 20 (2024) e02868

Contents lists available at ScienceDirect

Case Studies in Construction Materials

journal homepage: www.elsevier.com/locate/cscm

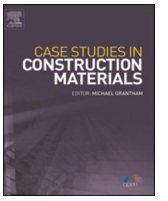

Case study

Analysis of the static and dynamic elastic moduli of a one-coat rendering mortar with laboratory and in situ samples

Guillermo Aragón [a], Heriberto Pérez-Acebo [b,*], Miguel Ángel Salas [c], Ángel Aragón-Torre [a]

[a] Department of Civil Engineering, University of Burgos, c/ Villadiego, s/n, 09001 Burgos, Spain
[b] Mechanical Engineering Department, University of the Basque Country UPV/EHU, Pº Rafael Moreno Pitxitxi, 2. 48013 Bilbao, Spain
[c] Department of Architectural Construction and Construction and Land Engineering, University of Burgos, c/Villadiego, s/n, 09001 Burgos, Spain

ARTICLE INFO

Keywords:
Rendering mortar
Dynamic elastic modulus
Static elastic modulus
Vibration mode
Masonry

ABSTRACT

Although the compressive strength is the most commonly used property to characterize mortars, it has limited representativeness in real-world applications. The deformation properties of mortars, specifically the elastic modulus, are responsible for masonry behavior. However, there is currently no standard method for determining the elastic modulus of mortars and no consensus on the best approach. Therefore, the aim of this paper is to obtain both static and dynamic moduli of a one-coat rendering mortar following the standards for calculating them on concrete specimens and verify their validity. The static modulus was determined under compression by adapting the standard for concrete specimens (EN-1352) to mortars using two gauges, and under the flexural tensile test following the standard EN-1015–11. The dynamic modulus was calculated by measuring the fundamental resonant frequencies of longitudinal and transverse vibration modes, adapting the American standard for concrete (ASTM C215) for mortar. The tests were performed on both standardized and non-standardized prismatic specimens, as well as in situ samples at various ages. The results indicated that dynamic modulus obtained from the longitudinal vibration mode was higher than that from the transverse mode, but differences were smaller using a uniaxial accelerometer than with a triaxial accelerometer. The dynamic modulus exhibited a slightly higher value and lower dispersion than the static modulus. Both moduli decreased with time and were easily correlated through linear regressions. Additionally, both moduli were correlated with flexural and compressive strength values. In situ samples had lower elastic moduli, but the compaction procedure in real works differs from laboratory tests. In summary, it was demonstrated that the procedures for calculating dynamic and static elastic moduli in concrete can be applied to mortar samples, and their effectiveness was confirmed.

1. Introduction

Mortar is a crucial element in masonry, which is a composite anisotropic material. Mortars can distribute stress uniformly, smooth block irregularities, and accommodate deformations associated with thermal expansions and shrinkage. The compressive strength,

* Corresponding author.
E-mail addresses: garagon@ubu.es (G. Aragón), heriberto.perez@ehu.eus (H. Pérez-Acebo), masalas@ubu.es (M.Á. Salas), aragont@ubu.es (Á. Aragón-Torre).

https://doi.org/10.1016/j.cscm.2024.e02868
Received 11 October 2023; Received in revised form 20 December 2023; Accepted 7 January 2024
Available online 11 January 2024

traditionally measured on cubic or cylindrical samples, has been considered the primary property of mortars. However, the compressive strength has low representativeness in real-world applications because mortar behaves differently when confined in masonry works compared to standard specimens [1]. Moreover, it has been observed that an increase in mortar compressive strength has a limited effect on the increase of masonry compressive strength [2–4]. On the contrary, mortars are known to play a key role in the deformation properties of masonry composites, responsible for the non-linear behavior of masonry [5–9]. When applied to joints, they affect the behavior of the masonry or brickworks [10]. Rendering mortars, on the other hand, must be compatible with the substrate to which they are applied (such as flat ceramic, brick, or concrete surfaces), since their performance depends on the ability to adapt to the substrate without cracking [11]. The mechanical behavior of mortar depends on its response (deformation) to applied loads, which can cause cracks if the rigidity is excessive. Therefore, it is important to standardize the mortars based on their deformation properties, particularly the elastic modulus, to ensure optimal performance. The elastic modulus, also known as the Young modulus, E, is defined as the ratio of stress to strain within the linear elastic range under varying tensional states.

Currently, there is a push to develop more efficient employment and management of limited natural resources. As a result, the construction and building sector is aiming to develop more sustainable construction materials [12–14]. Cementitious materials are a particularly important topic due to their significant carbon footprint. The main trends in producing these materials involve reducing energy consumption and incorporating recycled waste elements [15–18]. In the field of mortars, it is common to follow both trends [19–24]. Therefore, in addition to traditional mortar characterization, it is essential to calculate elastic properties, such as static and dynamic elastic modulus.

Nevertheless, there are few references in the literature regarding the determination of elastic moduli in mortars [7,8,25–28], particularly with in situ samples [29]. Additionally, the best method for determining elastic modulus [30] remains unclear, leading to inconsistent characterization results when comparing data from different studies. Typically, research on elastic moduli focuses on concrete [31–34]. Marques et al. [35] proposed an adapted methodology based on the standard procedure used for concrete samples (ISO 6784) [36], which was modified to suit the characteristics of mortar samples. Additionally, the elastic properties of mortar cannot be measured without damaging it once it has been placed in real works. Generally, static tests are conducted in a laboratory or values are estimated from strength values from cylindrical specimens by applying equations based on experimental data, which can lead to significant errors [37]. Another possibility is to apply reduced stress in dynamic load conditions (non-destructive test) to obtain the purely elastic effects of the material. The technique yields the static elastic modulus, E_s, which corresponds to the initial tangential modulus of the stress-strain curve.

Besides, during the first half of the 20th century, differential equations were proposed based on elasticity theory to approximate the solution for determining the elastic constants of samples with rectangular or cylindrical shapes vibrating with free edges [38]. These equations are applicable to isotropic and homogeneous media with specific shapes and boundary conditions. The equations were successfully employed for determining the dynamic elastic modulus using various test procedures. Among them, the excitement of the material sample by applying an impulse excitation of vibration has gained significant attention and has become the most widely used [39]. This procedure is similar to other standards and there are more references in the literature that employ this technique [6,7,25,33,37,40–43]. The elastic modulus calculated under dynamic conditions is known as the dynamic elastic modulus, E_d, defined as the ratio of stress to strain under vibratory conditions.

Furthermore, there is a noticeable gap in the bibliography regarding the correlation between the static and dynamic elastic modulus of mortars and other material properties. Therefore, research findings conducted with concrete samples are being applied to studies with mortars. For instance, some studies have correlated the compressive strength with ultrasonic wave propagation velocity for various concrete compositions [44,45]. In their analysis, Han and Kim [46] examined the influence of different factors on the relationship between static and dynamic elastic modulus, as well as between dynamic modulus and compressive strength in concrete. They found that for mortars, the dynamic moduli were slightly higher than the static modulus, and a correlation could be established for each type of specimen [47]. However, there has been little attention given to the correlation between static and dynamic elastic moduli for any type of mortar, and there are relatively few articles available on the subject in the literature.

Consequently, since there is no standard for determining the elastic modulus of mortars [30,35,42], this paper aims to obtain both static and dynamic moduli of a one-coat rendering mortar following the standards for calculating static and dynamic moduli of concrete samples [39,48]. Therefore, this methodology is proposed as a valid standard for determining the static and dynamic elastic moduli for mortar specimens. The article presents correlations between the static and dynamic modulus, which could assist practitioners in estimating the static modulus from the more readily available dynamic modulus. It also examines the correlations between both moduli and other mechanical properties, the evolution of the moduli over time, and the influence of thickness on the moduli.

2. Material and experimental program

2.1. Material

For this study, a commercially available one-coat rendering mortar was selected. These types of rendering mortars are currently produced and sold in 20–30 kg bags of dry product for use in construction and building. The cement used can be either gray or white Portland cement, and the aggregates consist of a mixture of rounded siliceous and crushed limestone particles with a size less than 2 mm. In addition, mineral additives, such as water retainers, light aggregates, waterproof agents, cellulose fibers, air-entrainment additives, color pigments, and polymeric micro-fibers, are commonly included in cements and other substances to enhance their performance [49,50]. The product only needs water to be added, and it is available in various colors.

The mortar selected for this project contains white Portland cement BL I/A-L 42.5 R, which is categorized according to the

European standard EN 998 [51] for masonry mortars. Specifically, EN-998–1 [52], the chapter on rendering mortars, uses three properties to categorize them: compressive strength, capillary absorption of water, and thermal conductivity. These properties are shown in Table 1. Other standards, such as BS 5628 [53], are also in use. According to the commercial product specifications, the mortar used in this study is classified as CS III W2 T2, which can be employed in rainy and cold conditions, for coating thicknesses between 15 and 20 mm. Additional characteristics of the mortar are presented in Table 2, and Table 3 shows the mortar mixtures as provided by the manufacturer. Additionally, a particle analysis of the mortar was performed, revealing a composition consistent with that of a cement-based material (Table 4).

2.2. Specimen preparation

The specimens were prepared according to the mixing procedure indicated in standard EN 196–1 [54], using a water proportion of 24%, as recommended by the mortar producer. After mixing enough mortar, it was placed in standardized molds with dimensions of 40 × 40 × 160 mm (thickness × width × length) [55].

To characterize the mortar, we conducted three series of specimens on different days, each with three mixing processes. Additionally, we conducted two more series to determine the dynamic elastic modulus using non-standardized dimensions of 15 × 40 × 160 mm and 20 × 40 × 160 mm. These samples were manufactured to be compared with the in situ samples. In total, 25 molds were filled on different days. The specimens were identified by two letters (MP) and two numbers ranging from 01 to 34. The letters A, B, or C were used to distinguish the specimens from each mold. In total, 75 specimens were produced, including 45 with standardized RILEM dimensions (40 × 40 × 160 mm), 15 with dimensions of 20 × 40 × 160 mm, and 15 with dimensions of 15 × 40 × 160 mm.

Finally, six specimens were extracted from a building where the same mortar was used and mixed under the same conditions. Three specimens, numbered 1 to 3, were obtained from each sample labeled E and F.

2.3. Experimental program

2.3.1. Flexural and compressive strength

The flexural tensile strength ($f_{m,t}$), or flexural strength as indicated in the standard, was obtained at 28 days using the prismatic 40 × 40 × 160 mm samples following the standard EN 1015–11, 1999 [55]. Additionally, the compressive strength ($f_{m,c}$) of hardened mortar at 28 days was also determined according to standard EN-1015–11, 1999 [55]. Compressive strength is commonly used to identify and prescribe mortar due to its importance and ease of measurement. Other characteristics can be deduced from this value. Samples for the compressive test were taken from the two halves of the prismatic sample resulting from the flexural test described earlier.

2.3.2. Adaptation of standardized tests to mortars

For a rendering mortar like the one analyzed in this study, it is crucial to obtain in situ values of the mechanical characteristics. This is because the thickness and curing time of the mortars differ from the dimensions and ages indicated in the reference standards for mortars, EN 1015 [55]. Additionally, non-destructive tests are necessary to determine the evolution of the elastic properties over time in the same specimen.

With this aim, the following procedure was included in the planning:

1. The static elastic modulus under compression was determined by adapting the standard for concrete specimens (EN-1352) [48] to mortars. To measure the deformations, two strain gauges were used in each sample, which were connected to an amplification and data acquisition module (HBM QuantumX 1615B) (Fig. 1a). Moreover, the static elastic modulus was calculated under flexural tensile test, as described in EN-1015-11 [55], using strain gauges as well (Fig. 1b). In the flexural test, samples were loaded until rupture.
2. The dynamic elastic properties were determined by analyzing the fundamental resonant frequencies following the test scheme proposed in the American standard for concrete [39].
3. The static bending (flexural) test described in Section 2.3.1 can be used to determine the (flexural) tensile static modulus and, in some cases, the compressive static modulus. During the test, the samples were equipped with two identical strain gauges on the upper face (under compression strain) and lower face (under tension) to measure deformation. By reading the values of these gauges and the applied loads, the strain-load curve of the material can be determined. The elastic modulus was determined by calculating the slope of the regression curve in the linear zone of the plot.

Table 1
Classification of the properties of the hardened mortar according to EN 998–1 [52].

Properties	Category	Values	Properties	Category	Values
Compressive strength after 28 days	CS I	0.4 – 2.5 N/mm^2	Capillary absorption of water	W 0	Not specified
	CS II	1.5 – 5.0 N/mm^2		W 1	C $\leq$ 0.40 kg/m^2 min$^{0.5}$
	CS III	3.5 – 7.5 N/mm^2		W 2	C $\leq$ 0.40 kg/m^2 min$^{0.5}$
	CS IV	$\geq$ 6.0 N/mm^2	Thermal conductivity	T 1	$\leq$ 0.1 W/m·K
				T2	$\leq$ 0.2 W/m·K

Table 2
Characteristics of the mortar facilitated by the manufacturer.

Characteristics	Value	Characteristics	
Mixing water [%]	24	Compressive strength after 28 days [MPa]	7.5
Water retention [%]	$\geq$ 90	Bending test strength after 28 days [MPa]	2.0
Consistency [mm]	148	Shrinkage after 28 days [mm/m]	0.9
In-fresh density [kg/m3]	1733	Dynamic elastic modulus [MPa]	6500
Bulk hardened density [kg/m3]	1512		

Table 3
Components of the mixture in the mortar, facilitated by the manufacturer.

Material	Quantity (% in weight)
White Portland cement BL I/A-L 42.5 R	21 $\pm$ 1
Siliceous and limestone aggregates	76 $\pm$ 1
Additives	3 $\pm$ 0.5

Table 4
Element analysis of the mortar.

Element	Percentage in weight (%)
C	20.32
Na	0.68
Al	1.51
Si	7.60
K	0.67
Ca	2.73
Fe	0.49
O	65.79

It should be noted that the first two points use non-destructive tests, except for the flexural test. Therefore, specimens can be employed for additional tests over time or for destructive tests. The results of both dynamic and static elasticity moduli are obtained under simplified hypotheses. The equations used to calculate the Young modulus are valid for isotropic and homogeneous media, which is not entirely true in the case of mortars.

As previously mentioned, the elastic modulus is calculated using standardized specimens with dimensions of 40 $\times$ 40 $\times$ 160 mm. In addition, specimens with the same length and width as the standardized ones, but with varying thicknesses (15 and 20 mm), were used to observe the influence of thickness on the results and to compare them with the values from in situ samples (Fig. 1c). The samples with the lowest thickness (15 and 20 mm) were not included in the compressive tests to determine the static modulus or the compressive tests with rupture, as described in Section 2.3.1. This was due to the small size of the samples and the lack of equations to compare them with the normalized tests. Table 5 summarizes all of the manufactured samples, the tests conducted on them, and the age at which they were tested. Fig. 1d presents a scheme of the conducted tests and the results (elastic moduli and strengths) that are determined in each test.

2.4. Numerical simulation of the dynamic deformation modulus

To accurately identify the frequencies associated with each vibration mode, a numerical simulation was performed using a finite element method program. This allowed for verification of the behavior of specimens with varying dimensions (40 $\times$ 40 $\times$ 160 mm, 20 $\times$ 40 $\times$ 160 mm, and 15 $\times$ 40 $\times$ 160 mm) when excited by an impact vibration (pulse). The material was characterized by a density of 1550 kg/m^3. The adopted values for the elastic modulus and Poisson coefficient were 5500 MPa and 0.20, respectively. These values are consistent with laboratory observations and enable the development of an approximate model.

The model included a mesh of hexahedral 8-noded elements with a maximum length of 2 mm and was parameterized to adapt to the proposed dimensions. This allows for the deduction of all vibration models of the prismatic samples in the study, including the longitudinal, transversal, and torsional vibration modes and their respective resonant frequencies.

3. Determination of mortar elastic properties

3.1. Elastic modulus (E_s)

3.1.1. Determination of the static elastic modulus under compression load

It was decided to obtain the E_s following the standard for determining the static elastic modulus under compression load for concrete (EN-1352, 1997) [48] with mortar samples, following other researches [56] because there is no standard about it. Therefore,

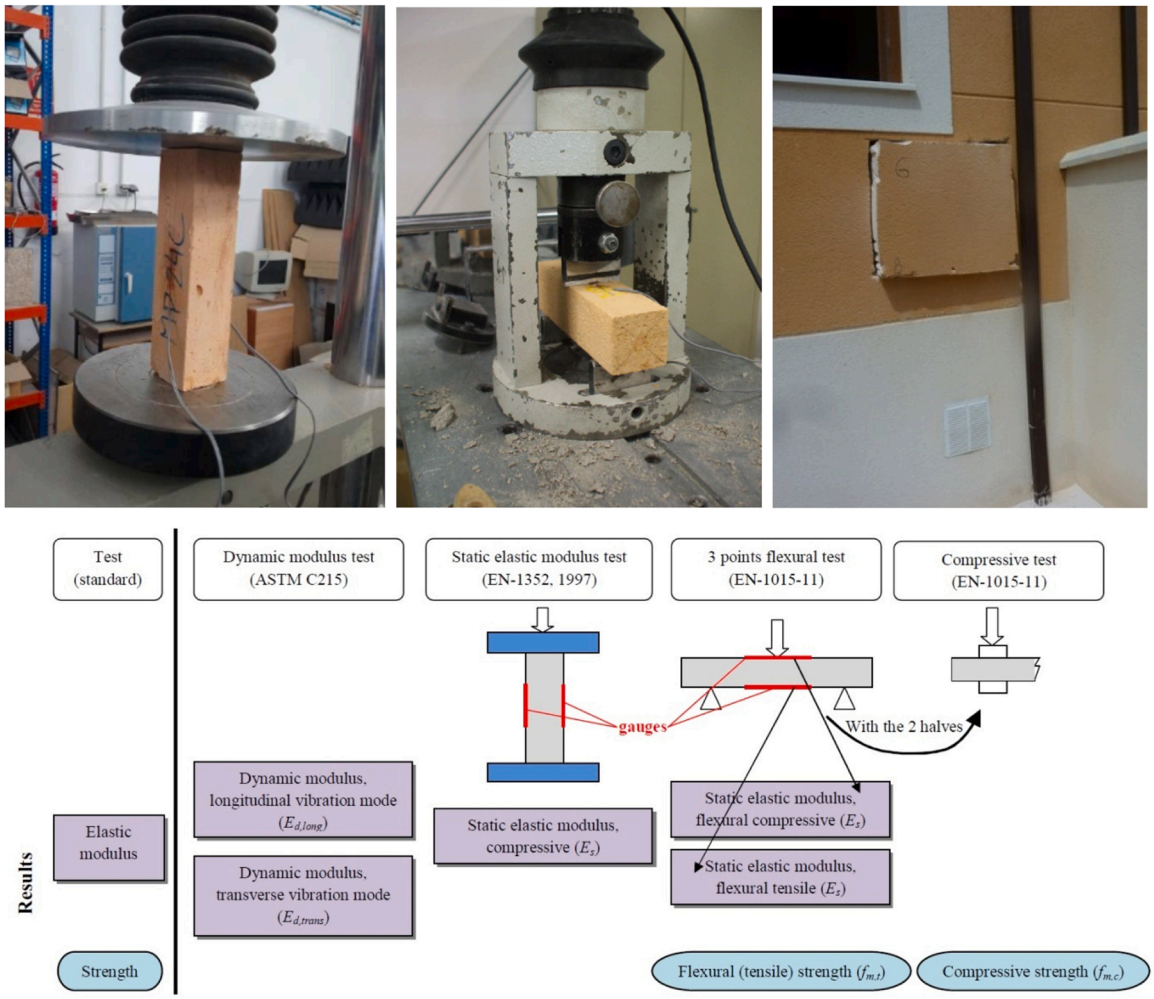

Fig. 1. (a) Compressive test, (b) Flexural test, (c) Extracting in situ samples, (d) Scheme of tests and obtained results (elastic moduli and strengths).

it is a non-standardized test and its aim is to obtain a reference value when calculating the dynamic modulus. In this standard, the static elastic modulus (E_s) is calculated from the difference between the longitudinal strain differences corresponding to a compressive stress from the beginning of the test (approximately 5% of the observed compressive strength), σ_a, to a maximum stress of the test, σ_b, (which is generally about 1/3 of the maximum compressive strength of the material). Thus, the static modulus is calculated according to Eq. (1),

$$E_s = \frac{\Delta\sigma}{\Delta\varepsilon} = \frac{\sigma_b - \sigma_a}{\varepsilon_b - \varepsilon_a} \tag{1}$$

where E_s is the static elastic modulus [MPa]; σ_b is the maximum test stress after the last load cycle [MPa]; σ_a is the initial test stress before the last load cycle [MPa]; ε_b is the average strain corresponding to the maximum test stress σ_b; ε_a is the average strain corresponding to the initial test stress σ_a.

It was preferred to measure the short deformations with strain gauges because they are more sensitive to the small deformation in each load step (Fig. 1a).

3.1.2. *Determination of the static elastic modulus from flexural tensile test*

The static modulus was determined by measuring the sample deformation using strain gauges during the flexural test, following the procedure in standard EN-1015–11 [55] and other researchers' work [42]. The test followed the classic three-point flexural test for determining flexural strength (Fig. 1b). The only difference is the placement of two strain gauges, which are placed on the tensile face and on the compressive face (Fig. 1d). This placement allows for the plotting of strain-deformation graphs for the material, which were also used to calculate the mortar's static elastic modulus (E_s). The samples were tested until rupture, as previously mentioned.

Table 5
Test planning.

Sample	Dimensions (mm)	Age [days]					
		Elastic modulus				Destructive tests	
		Dynamic		Static		Flexural tensile test	Compressive test
		Longitudinal	Flexural	Compressive	Flexural (destr.*)		
MP01	40 × 40 × 160			28	28	28	28
MP02	40 × 40 × 160				28	28	28
MP03	40 × 40 × 160	77 329	77 329	329	329	329	329
MP04	40 × 40 × 160	77 364	77 364	364	364	364	364
MP05	15 × 40 × 160	364	364		364	364	
MP06	20 × 40 × 160	364	364		364	364	
MP07	40 × 40 × 160				28	28	28
MP08	40 × 40 × 160				28	28	28
MP09	40 × 40 × 160	70 147	70 147	147	147	147	147
MP10	40 × 40 × 160	70 182	70 182	182	182	182	182
MP13	40 × 40 × 160			28	28	28	28
MP14	40 × 40 × 160			28	28	28	28
MP15	40 × 40 × 160	42 91	42 91	91	91	91	91
MP16	40 × 40 × 160	42 119	42 119	119	119	119	119
MP19	20 × 40 × 160	28	28		28	28	
MP20	15 × 40 × 160	28	28		28	28	
MP21	20 × 40 × 160	28 56 84	28 56 84		84	84	
MP22	15 × 40 × 160	28 56 84	28 56 84		84	84	
MP23	40 × 40 × 160	28 56	28 56	56	56	56	56
MP24	40 × 40 × 160	28 56 84	28 56 84	84	84	84	84
MP27	20 × 40 × 160	28 105	28 105		112	112	
MP28	15 × 40 × 160	28 105	28 105		112	112	
MP29	20 × 40 × 160	28 56	28 56		56	56	
MP30	15 × 40 × 160	28 56	28 56		56	56	
MP32	40 × 40 × 160	28 42 112	28 42 112	112	112	112	112

* Note: The flexural test for determining the static elastic modulus is a destructive test

3.2. Determination of the dynamic modulus

Standards exist to determine the dynamic elastic modulus for certain materials, including concrete, natural stone, and refractory products, through the application of resonant frequency analysis techniques. Nonetheless, there is currently no specific standard for calculating the dynamic elastic modulus of mortars. In fact, there is no standard for calculating the elastic modulus of mortars [42]. Therefore, it was decided to follow the American standard for concrete (ASTM C215) [39], adapting it to mortar samples. This procedure is identical to the FEM simulation, and the results can be compared with those of other researchers in the literature [6,25,33,37,40–43,57]. The procedures developed for other materials, such as natural stone [58] or refractory products [59], are similar and yield comparable results to the concrete standard [39].

Dynamic tests offer an additional advantage as they are non-destructive [60,61]. This means that samples can be used to track the evolution of properties over time or for other destructive tests. The procedure allows for the measurement of mortar elasticity without damaging the specimen, providing a wide range of data for statistical purposes. This enhances the accuracy and consistency of the results.

The test measures the longitudinal vibration mode (tensile/pure compression), the transverse or bending vibration modes, and torsional mode. To achieve this, an instantaneous impulse is applied to the sample using a hammer, and the resulting signal or frequency spectrum is recorded. Using these measures, and taking into account the geometry and density of the specimens, it is possible to calculate the dynamic elastic modulus for the longitudinal fundamental vibration mode ($E_{d,long}$), for the transverse or bending fundamental vibration mode ($E_{d,trans}$), the dynamic transverse deformation modulus (G), and the Poisson coefficient (ν).

In accordance with the standard [39] for determining resonant frequency through impact, the following devices were utilized:

a) A Brüel &Kjaer 2302-5 (SN) hammer with a rubber handle and steel sphere head, equipped with a load cellule
b) A signal transducer. The more accurate transducer is a piezoelectric accelerometer with a resonant frequency of, at least, twice the maximum frequency of the operation. Two accelerometers were used: 1) a uniaxial accelerometer 4519-003 of 1.5 g of mass, with an operation frequency range between 0.5 and 20,000 Hz and a sensitivity of 10 mV/g; and 2) a triaxial 4524B of 100 mV/g and a weight of 4.8 g.
c) A frequency digital analyzer, which was connected to the hammer and the accelerometer. This analyzer consisted on a signal amplifier and software that analyzed the response from the transducer and converted it into a frequency spectrum.
d) Frames, serving an important function by isolating the samples from outside vibrations. If frames are rigid and are placed in the nodes, they can define the vibration modes.

The device scheme used for conducting the test is shown in Fig. 2, as presented in [39]. Before conducting the tests, a verification of the measuring chain was performed.

3.2.1. Dynamic elastic modulus from the longitudinal vibration mode ($E_{d,long}$)

The dynamic longitudinal elastic modulus was calculated using the fundamental vibration frequency, determined by the resonance method by impact, according to section 9.2 of the ASTM-C215 standard [39]. Fig. 3a) shows the load application scheme and the accelerometer placement, while Fig. 4a) shows the test procedure.

The dynamic longitudinal elastic modulus ($E_{d,long}$) is calculated by Eq. (2), proposed in ASTM-C215 [39]:

$$E_{d,long} = D \cdot M \cdot (n')^2 \cdot 10^{-6} \tag{2}$$

Where $E_{d,long}$ is the dynamic elastic modulus from the longitudinal vibration mode [MPa]; M is the mass of the sample [kg]; n' is the longitudinal frequency [Hz]; D is a coefficient, with a value for prismatic samples of (Eq. 3),

$$D = \frac{4 \cdot L}{b \cdot t} \tag{3}$$

where L is the length [m], b is the width [m], and t is the thickness [m] of the sample. After introducing the sample dimensions, it results in Eq. (4):

$$E_{d,long} = 4 \cdot \frac{L}{b \cdot t} \cdot M \cdot (n')^2 \cdot 10^{-6} \tag{4}$$

3.2.2. Dynamic elastic modulus from the transverse mode ($E_{d,trans}$)

The frequency of the flexural vibration mode was determined using the same resonance technique by impact, as described in section 9.1 of [39]. The device and procedure were similar, with differences only in the sample support, accelerometer placement (if using a uniaxial accelerometer), and impact point (Fig. 3b). Once the samples were supported by the frames and could vibrate freely in transverse mode, the impact was applied at the central point of one of the lateral sides of the samples, as shown in Fig. 4b. The nodes were placed at a distance of 0.224 times the length of the sample (approximately one-fourth of the distance). Section 10.1 of the ASTM C215 standard [39] provides Eq. (5) to determine the dynamic modulus from the fundamental transverse resonant frequency, $E_{d,trans}$ [MPa].

$$E_{d,trans}[MPa] = C \cdot M \cdot n^2 \cdot 10^{-6} \tag{5}$$

Where M is the mass of the specimen [kg], n is the transverse frequency [Hz], and C is a coefficient, which considers the geometry of the sample. For the standardized prismatic samples, Eq. (5) is converted to Eq. (6),

$$E_{d,trans}[MPa] = 0.9464 \cdot \frac{L^3 \cdot T}{b \cdot t^3} \cdot M \cdot n^2 \cdot 10^{-6} \tag{6}$$

where L is the length, b is the width and t is the thickness of the samples, all expressed in [m]; and T is the correction factor, which depends on the relationship between the turning radius (denominated K) and the length of the sample (L), and the Poisson coefficient (ν).

3.2.3. Dynamic elastic modulus from the torsional mode

The fundamental torsional frequency was determined using the resonance technique described in section 9.3 of [39]. The devices used for measuring this frequency were the same as those used for measuring other vibration modes, with the only difference being the position of the accelerometer and the impact point (Fig. 3c and Fig. 4c). Eq. (7) in section 10.3 of [39] can be used to calculate the dynamic rigidity modulus, G_d, from the fundamental torsional frequency.

$$G_d[MPa] = B \cdot M \cdot (n'')^2 \tag{7}$$

Where M is the sample mass [kg], n'' is the torsional frequency [Hz] and B is defined by Eq. (8):

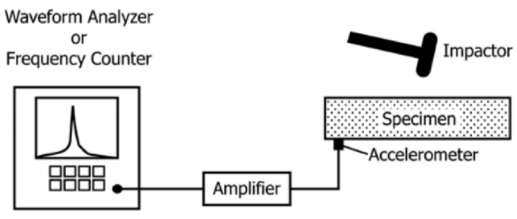

Fig. 2. Devices for the impact based resonance method test.

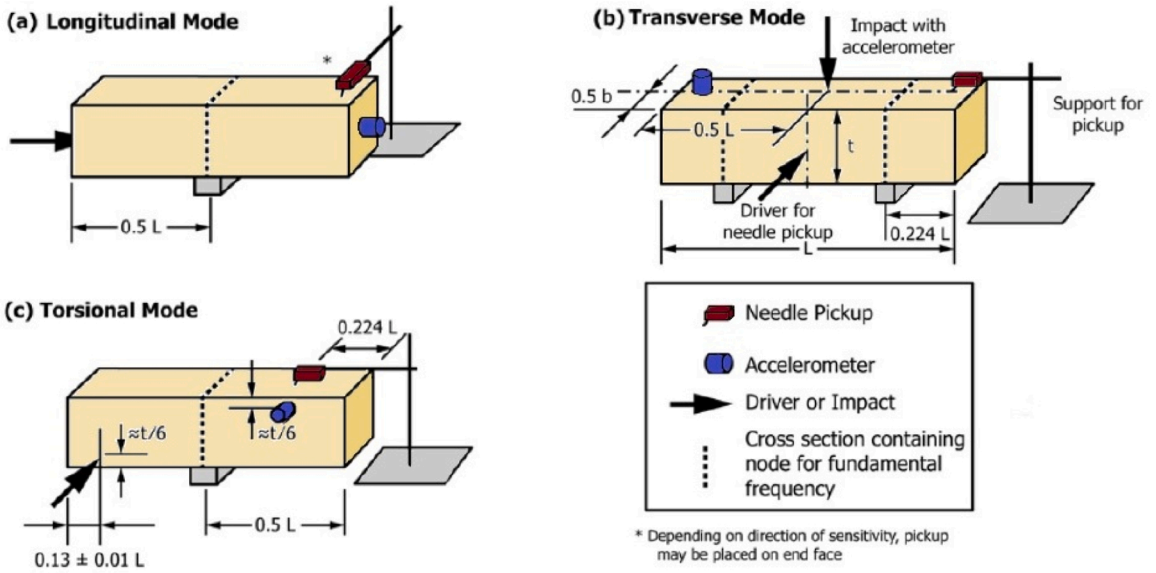

Fig. 3. Scheme of the test procedure for each mode of vibration, (a) longitudinal mode, (b) transverse mode, and (c) torsional mode.

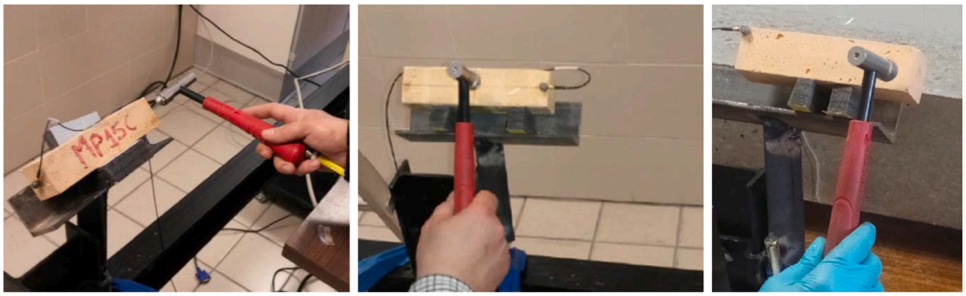

Fig. 4. Tests conducted at the laboratory, (a), longitudinal mode of vibration, (b) transverse mode of vibration, and (c) torsional mode of vibration.

$$B[m^{-1}] = \frac{4 \cdot L \cdot R}{A} \tag{8}$$

Where L is the sample length [m], A is the area of the transverse section of the sample [m^2], and R is a shape factor, and for a prismatic sample whose dimensions are b and t, defined as before, with $t > b$, is defined by Eq. (9),

$$R = \frac{\frac{t}{b} + \frac{b}{t}}{\frac{4t}{b} - 2.52 \cdot \left(\frac{t}{b}\right)^2 + 0.21 \cdot \left(\frac{t}{b}\right)^6} \tag{9}$$

For a prismatic sample with a squared section R = 1.183.

3.2.4. Poisson coefficient

All parameters required for calculating the elastic modulus can be obtained through direct measurement or dynamic methods. The length (L), width (b), and thickness (t) can be directly measured, while the mass can be weighed with precision. The fundamental vibration frequencies for each mode can be determined using the vibration method as described. The Poisson coefficient is the only characteristic that cannot be directly measured, but there are two methods available to obtain it.

1) In order to determine the Poisson coefficient for one-coat or rendering mortars, it is recommended to consult scientific literature. If a specific value cannot be found, a general value for mortar can be used as the coefficients for these materials are very similar. It is important to note that these values are approximations and may result in a small error when determining the dynamic modulus. For lime and cement mortars, a value of 0.22 [42] or for masonry mortars, a value of 0.20 [25] can be used.
2) The Poisson coefficient, which represents the relationship between the lateral and longitudinal deformation for an isotropic material, can be calculated using Eq. (10) in section 10.4 of [39].

$$\nu = \frac{E_{d,long}}{2 \cdot G} - 1 \tag{10}$$

where $E_{d,long}$ is the longitudinal dynamic elastic modulus [MPa], and G is the dynamic rigidity modulus [MPa].

4. Numerical simulation

The use of finite element method (FEM) based analysis software proved to be beneficial. The specimen dimensions were reproducible, and the software provided resonant frequency ranges that were easily identifiable during testing. Fig. 5 presents the simulated vibration modes for prismatic specimens with dimensions of 40 × 40 × 160 mm. The FEM software was used to create a calculation routine that correlates expected frequencies with material elastic properties (Fig. 6). This allowed for quick comparison of the test data. A density of 1500 kg/m^3 and a Poisson coefficient of 0.20 were adopted.

For the analyzed data, higher frequencies were obtained for the longitudinal vibration mode within a dynamic modulus range of 4000 to 8000 MPa. These numerical simulation results confirm the adequacy of Eqs. (2), (5), and (7), which show a parabolic relationship between the frequencies and the dynamic modulus. It is important to note that the dynamic modulus only depends on the square of the resonant frequency as long as the geometrical and material data remain constant. The frequencies for the transverse vibration mode range from 2215 to 3131 Hz, while for the longitudinal mode, they range from 5092 to 7202 Hz. It is expected that there will be a higher deviation in data from the piezoelectric accelerometer at higher frequencies due to device accuracy, as with any measurement.

Fig. 7 illustrates the correlation between the dynamic elastic modulus for the transverse vibration mode and the fundamental resonant frequency for specimens with dimensions of 40 × 160 mm and varying thicknesses. The results indicate that higher thicknesses require higher frequencies and frequency ranges to achieve the same dynamic modulus. The validity of Eq. (6) was once again confirmed through numerical simulation.

5. Results and discussion

As previously stated, all analyzed specimens were manufactured using the same product: an industrially produced one-coat rendering mortar, mixed with water in a proportion of 24% of the weight of the mortar, as specified by the manufacturer. The standardized mixing procedure [62] and curing procedure [55] were followed, ensuring that all mixtures had the same component proportions. When determining all the elastic properties of the material, changes in the results could be related to the age, specimen dimensions, and type of test. The values were mostly obtained at 28 days, which is the usual age for mortar prescriptions. Nevertheless, tests were conducted at variable ages, with a maximum of 364 days.

5.1. Flexural and compressive strength

Some flexural and compressive tests were conducted on normalized samples (40 × 40 × 160 mm) after 28 days (Table 6). The average flexural strength ($f_{m,t}$) at 28 days was found to be 2.72 MPa, and the average compressive strength was 7.20 MPa. The results

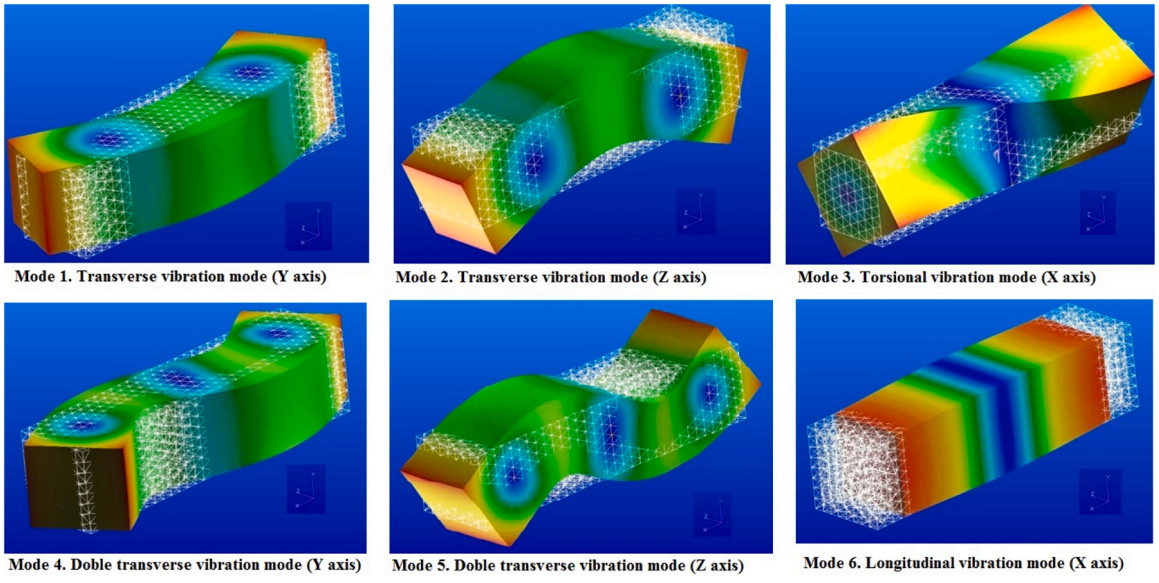

Fig. 5. Vibration modes for the standardized prismatic specimen (40 × 40 × 160 mm).

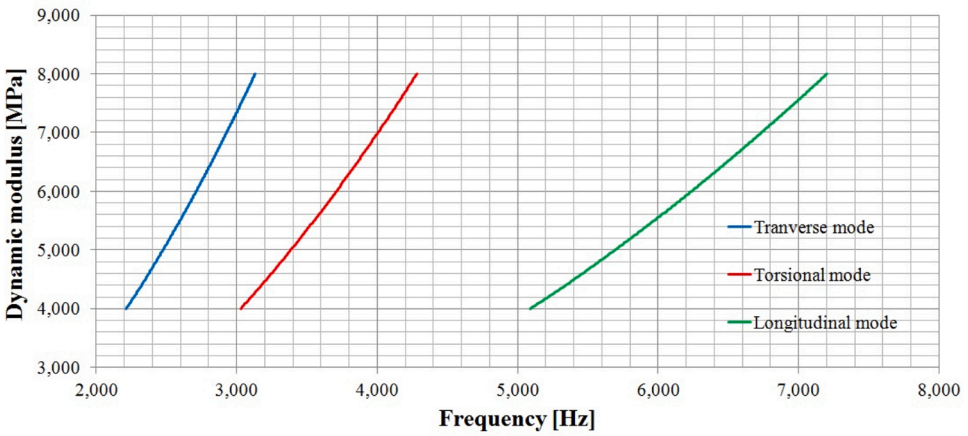

Fig. 6. Variation of the dynamic modulus and G for each vibration mode for each resonant frequency.

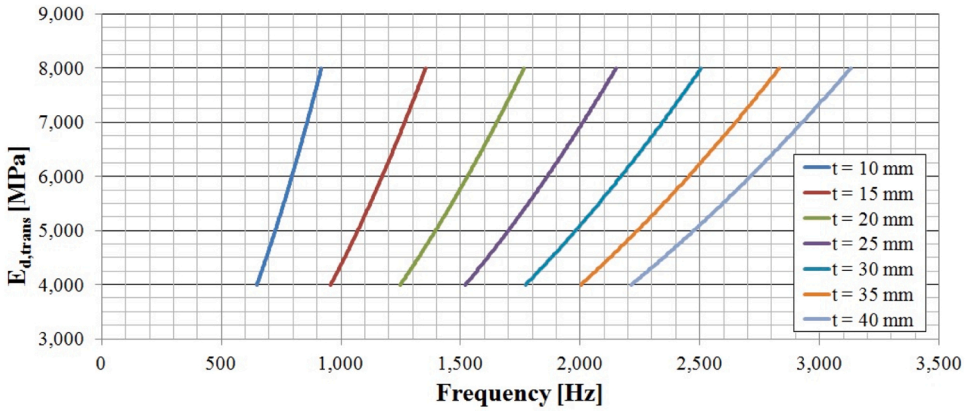

Fig. 7. Variation of the dynamic elastic modulus in transverse mode as a function of the frequency and specimen thickness.

are well correlated, and if one value is known, the other can be easily deduced (Fig. 8).

Haach et al. [63] proposed that the flexural strength is approximately one-third (0.30–0.34) of the compressive strength. If we remove the intercept in the equation shown in Fig. 8, we obtain a coefficient value of 0.377 for 'x', with a determination coefficient (R^2) of 0.918. Therefore, the obtained equation is similar to those found in the literature.

Additional specimens underwent flexural and compressive testing at various ages. Fig. 9 illustrates the development of compressive and tensile (flexural) strengths over time for normalized specimens.

Both the compressive and tensile strengths decreased over time, with the compressive strength decreasing at a higher rate. Similar results were found when considering variable humidity and curing time [64,65]. Typically, the evolution of these strengths is only analyzed up to 28 days, during which they increase [22–24,66]. However, improvements in both strengths have been observed between 28 and 56 days [67,68]. Dawood et al. [69] conducted tests on samples at 90 days and found a 13% increase in compressive strength and a 6% increase in flexural strength compared to values at 28 days. Valentini et al. [26] reported similar results. Haach et al. [7] extended their analysis to 120 days and observed lower strength values at intermediate points (60 and 90 days) despite an overall

Table 6
Mortar flexural and compressive strength at 28 days.

Sample	Flexural strength ($f_{m,t}$) [MPa]	Compressive strength ($f_{m,c}$) [MPa]
PM01	2.7	7.4
PM02	2.7	7.2
PM07	2.6	7.0
PM08	2.3	6.2
PM13	3.1	8.0
PM14	2.9	7.4
Average values	2.72	7.20

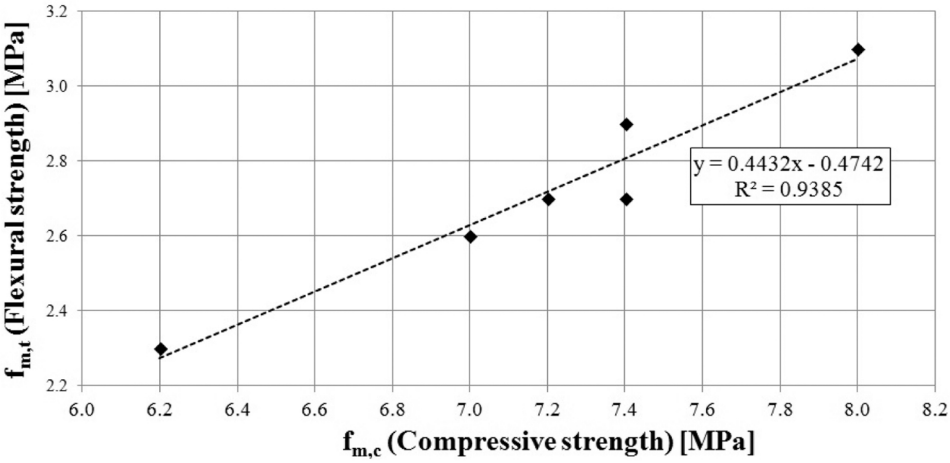

Fig. 8. Comparison of the flexural and compressive strength at 28 days.

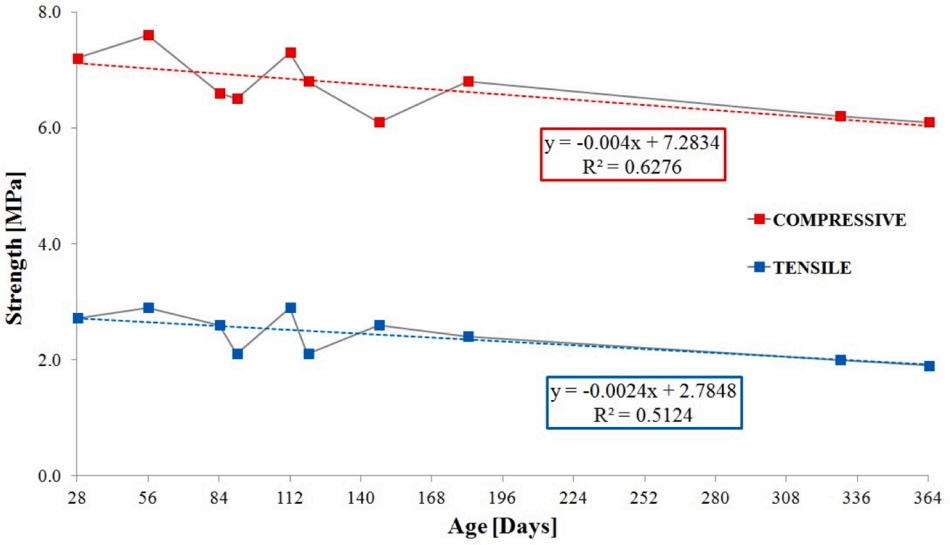

Fig. 9. Mortar compressive and flexural tensile strength evolution with time.

increase from 28 to 120 days, indicating variability in the strength data over time. Fig. 9 shows a slight increase in strength values up to 90 days, followed by a decrease at longer times. This trend is due to the loss of internal water during the curing process, resulting in a more porous and less compact material, which leads to a reduction in strength [70].

The impact of humidity loss during the process can have varying effects depending on the material characteristics. If the cement rate is low, curing shrinkage increases due to a lower tensile strength of the mortar, resulting in lower mechanical properties [71]. Furthermore, the use of superabsorbent polymers creates a more porous microstructure over time [72]. All of these factors influence the performance shown in Fig. 9.

5.2. Static elastic modulus

The standard for determining the static elastic modulus (E_s) under normalized compressive strength was followed [48], adapted to mortar specimens of 40 × 40 × 160 mm (Fig. 1a). Additionally, the flexural test at 3 points [55] was employed to determine the E_s, too.

The results of the static modulus calculation from the tensile face on the flexural test at 3 points with the 3 specimens of the PM09 series are shown in Fig. 10a. The load cell and gauge data from the tensile face were used for the calculation. The flexural moment is calculated using the load value and the distance between supports. This method allows for the deduction of the tensile strength in the extreme fiber, where the gauge is placed. Fig. 10b displays the same values, but for the compressive face.

To calculate the tangent of the curve, which represents the static modulus, it was preferable to obtain a high determination coefficient (R^2) with values close to one. This ensured a more accurate value. Good values of R^2 indicated a high linear correlation between the variables (stress and strain), which implied an elastic behavior of the material. After analyzing the strain-stress curves in Fig. 10a and Fig. 10b, it could be concluded that the mortar used had a longer elastic span than what is typically expected from traditional mortar [66]. Additionally, it had a lower rigidity and exhibits a characteristic fragile or quasi-fragile rupture without plastic behavior.

Fig. 11 compares the static modulus of mortar in standardized specimens tested under compressive and flexural conditions. Each point represents the average value of all specimens tested at a specific age.

Haach et al. [7] demonstrated that for certain mixtures, the static modulus remained nearly constant from 28 to 120 days, while in other mixtures, a noticeable increase was observed. Despite the initial phase's data dispersion (up to 90 days), which is expected from static tests, the elastic modulus decreased over time, as observed in other studies with mortar samples over the long term, up to one year [35]. The reason for this phenomenon is the same as for the decrease in flexural and compressive strength: the loss of internal water during the curing process, resulting in a more porous material. Additionally, there is an approximate correlation between the static elastic modulus obtained from the compressive test [48] and the one calculated from the flexural test on the upper face of the sample [55], with both values falling within the range of 5100 MPa. However, when a strain gauge is placed on the tensile face (lower face) of the bending test, it leads to higher values of the static elastic modulus, approximately 6000 MPa. This is because the strain gauge acts as reinforcement, similar to a bar in reinforced concrete, which increases the strength of the samples. This behavior is also observed in the E_s values calculated using data from the tensile face of specimens with varying thickness (Fig. 12). Since the gauge is identical, a lower thickness indicates higher strains in the mortar, resulting in a higher static modulus.

In Fig. 12, there is a dispersion of values ranging from 28 days to 90–100 days due to the low quantity of samples for each age. However, the values at one year clearly indicate a decreasing trend for the static modulus (obtained from flexural tensile data), with a variation between 11% and 16%. This is similar to other authors who found decreases in the Young modulus of up to 15% and 18%, depending on the water/cement ratio and age of the sample [71]. Although the R^2 values of the equations related to time proposed in Fig. 11 and Fig. 12 are not high, the purpose of these figures is to demonstrate the decreasing trend with time. For a more comprehensive analysis, additional samples should be tested. Additionally, it must be noted that the equations are only valid for a specific type of mortar.

Finally, when comparing the static deformation modulus with the strengths for normalized samples (40 × 40 × 160 mm); higher moduli wre obtained in specimens with greater flexural and compressive strengths (Fig. 13a and b). Although there is typically a high degree of variability in the data relating to elastic modulus and strength [26], good correlations were achieved, with R^2 values around 0.70. Potential relationships between compressive strength and static modulus have been previously presented [73]. Haach et al. [63] proposed equations with determination coefficients of 0.65 and 0.74, which were improved to 0.95 [25] and 0.99 [26] for cylindrical samples. Carrasco et al. [27] established a linear correlation with an R^2 value of 0.94. The equations in Fig. 13a and Fig. 13b demonstrated a strong correlation between static modulus and strength. However, it must be noted that these equations are empirical and should be used with caution when dealing with different types of mortar.

5.3. Dynamic elastic modulus

5.3.1. Dynamic elastic modulus calculation from tests

The procedure selected was proposed by the manufacturer and is detailed in the ASTM standard for concrete [39]. Two types of piezoelectric accelerometers (uniaxial and triaxial) were employed to improve test performance. The procedure was repeated at different ages as it is a non-destructive test and a sufficient number of specimens were available. However, the data from each

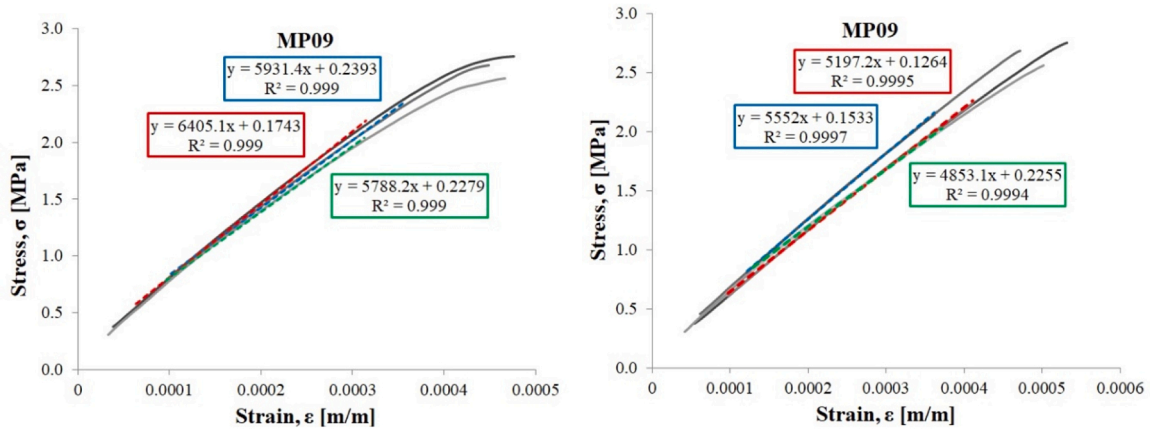

Fig. 10. Static elastic modulus calculation with values (a) from the tensile face during the flexural test; (b) from the compressive face during the flexural test.

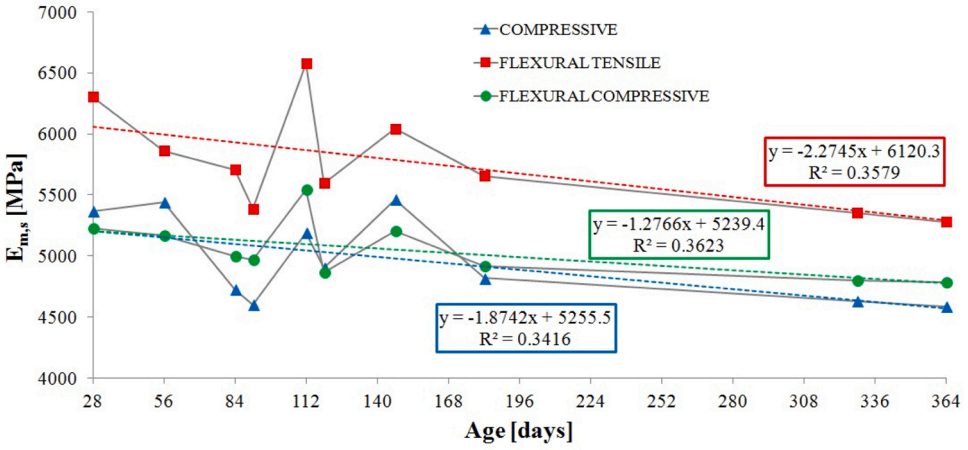

Fig. 11. Evolution of the static elastic modulus of standardized samples with time depending on the test.

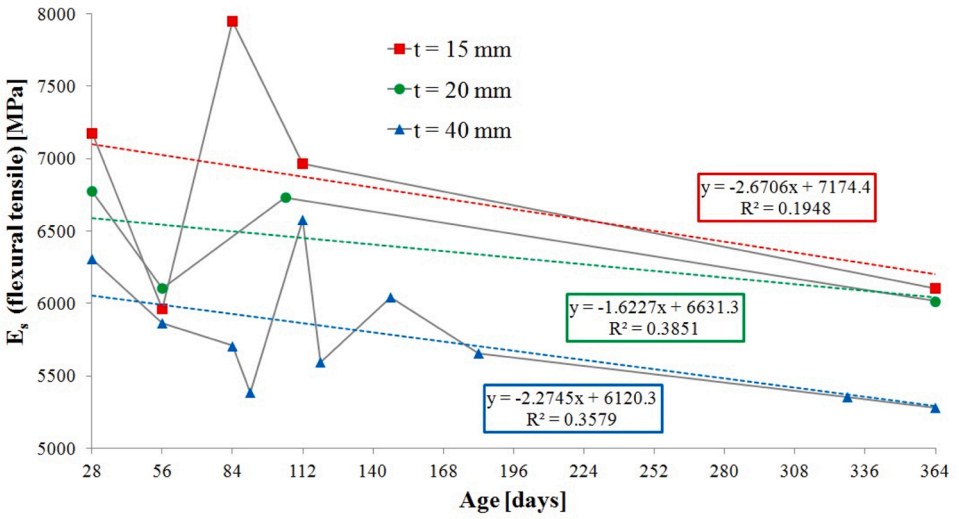

Fig. 12. Static modulus at different ages calculated from the tensile face in the flexural tests with various thicknesses.

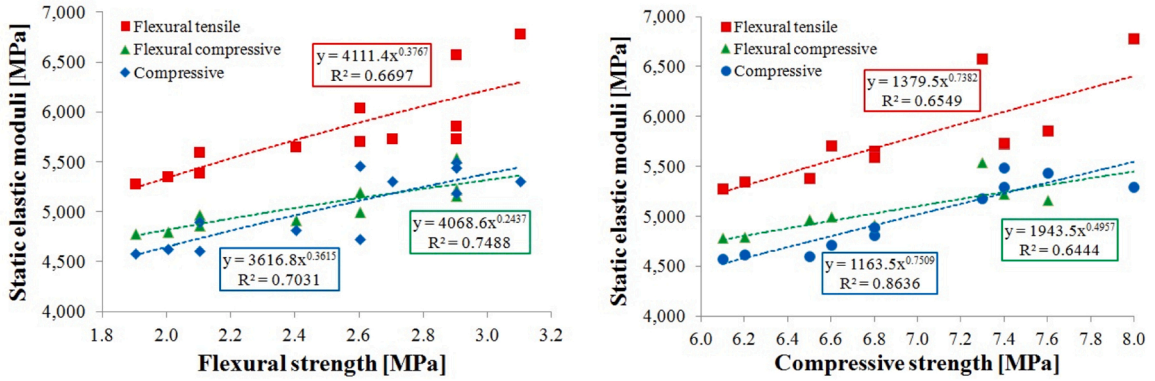

Fig. 13. Comparison between static elastic modulus and (a) flexural strengths, (b) compressive strengths.

accelerometer differed, requiring further analysis.

Fig. 14a displays the dynamic elastic modulus values, calculated according to standard [39], obtained from the fundamental frequencies of the longitudinal (Fig. 4a) and transverse vibration modes (Fig. 4b) using the uniaxial accelerometer. Each point represents the average value of the three specimens.

As shown in Fig. 14a, the dynamic modulus values were nearly identical for both vibration modes when measured with a uniaxial accelerometer. The longitudinal modulus was only slightly higher, by less than 1%. However, there was a strong correlation between the two values with low dispersion. The final average values for $E_{d,long}$ and $E_{d,trans}$ were 5401 MPa and 5348 MPa, respectively.

Values obtained from other studies on prismatic mortar specimens cured in a laboratory showed a similar trend, with variations ranging from 5% to 8% depending on the age. These values were obtained through the measurement of ultrasonic impulse velocity [64]. Notably, dynamic moduli obtained from ultrasonic impulses were higher than those obtained from impact vibration [42]. Other authors have reported slightly higher values for the dynamic transverse modulus ($E_{d,trans}$), approximately 4% higher, but these tests were conducted on cylindrical samples [25,37]. In some cases, the tests were conducted with very high accuracy ($R^2 = 0.9987$) [7]. Even higher differences, up to 45%, were observed for concrete with replacements of siliceous aggregates [74].

Tests were conducted using the triaxial accelerometer in Fig. 14b. This device has the advantage of obtaining both frequencies by only changing the place of load impact, without replacing the accelerometer, resulting in shorter laboratory test times. The longitudinal dynamic modulus was slightly higher than the transverse modulus, which was also observed in other works [42], with a variation of around 14%. Additionally, the correlation between them was lower (Fig. 14b). The average values for $E_{d,long}$ and $E_{d,trans}$ were 5957 MPa and 5124 MPa, respectively.

Some authors proposed adopting the average value of both moduli (obtained from transverse and longitudinal vibration frequencies) [42]. Following this suggestion, the dynamic deformation modulus of the mortar will be around 5500 MPa, regardless of the transducer employed. A deeper analysis of the values in Fig. 14b, classified according to the thickness of the specimens, yields Fig. 15. It should be noted that when calculating the dynamic transverse modulus, the smallest specimens were placed on the thickest face, where their rigidity is lower. This position causes the specimens to be excited at their lowest frequency, which becomes even lower as the thickness decreases. However, the longitudinal resonant frequency remains approximately the same for all cases. When specimens are separated by thickness, higher correlations between the dynamic moduli obtained from transversal and longitudinal modes are observed. The R^2 values are around 0.97 for specimens with a thickness of 15 cm and 20 cm.

Fig. 16 displays the resonant frequencies of prismatic specimens with varying thicknesses of 40 mm, 20 mm, and 15 mm.

The dotted lines represent the frequencies calculated using the FEM software, indicating similar moduli for both vibration modes. The lowest frequencies correspond to the thickest samples, where greater differences were found between the dynamic moduli calculated from the longitudinal and transverse modes. Higher accuracy (higher R^2) could be achieved if the equations in Fig. 16 included the intercept. However, for comparison with the values from the numerical simulation (dotted line), it was preferred to maintain them without the intercept. As observed, further research is necessary to understand the relationship between specimen dimensions, particularly sample thickness, vibration mode used to excite the samples, and test configuration.

In laboratory conditions with constant temperature and humidity, both the longitudinal and transverse dynamic moduli tended to decrease with age [75], as shown in Fig. 17, where each value represents the average value of the specimens at that age. The decreasing trend for both dynamic moduli is best represented by logarithmic curves, which have good correlation values.

Similar to the evolution of the strengths, this trend is related to the reduction of moisture content and changes in the microstructure [76]. The loss of water in the porous structure of the system relaxes the hydrostatic pressure and leads to a decrease in the elastic modulus of the mortar. This decrease is accelerated by cracking due to shrinkage. Cracks tend to appear more frequently in the transverse direction, which can have a greater impact on frequency measurement [77].

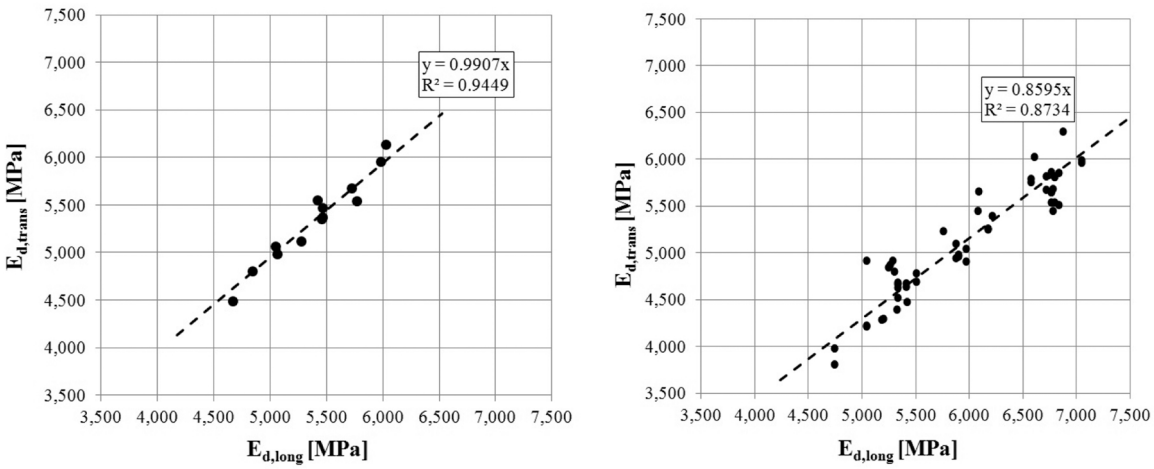

Fig. 14. a. Comparison of the dynamic modulus values from the longitudinal and the transverse vibration mode (a) with the uniaxial accelerometer, (b) with the triaxial accelerometer.

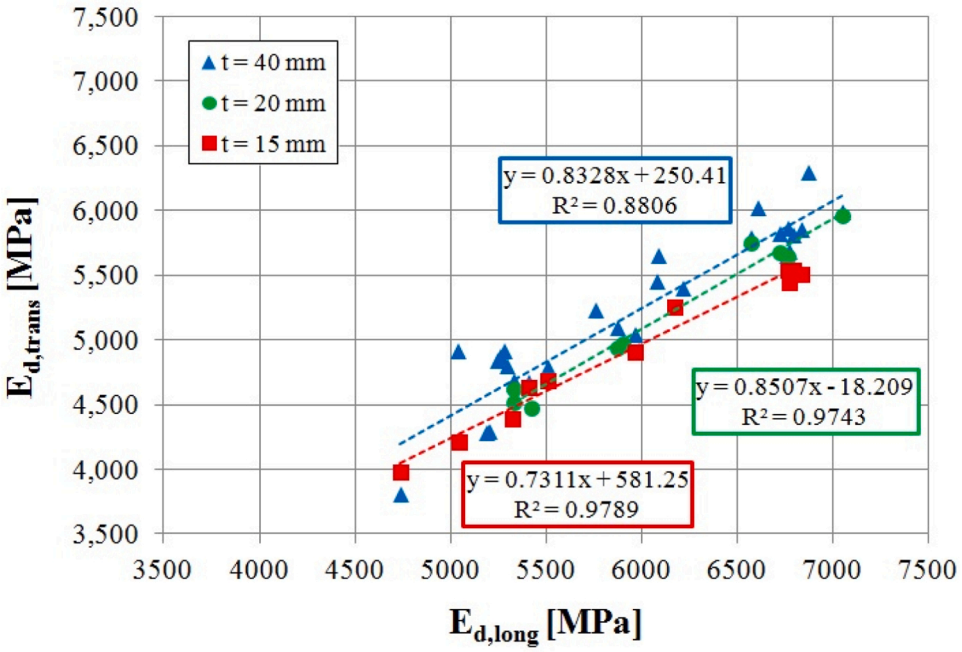

Fig. 15. Comparison of the dynamic modulus values from the longitudinal and the transverse vibration mode with the triaxial accelerometer for various specimen thickness.

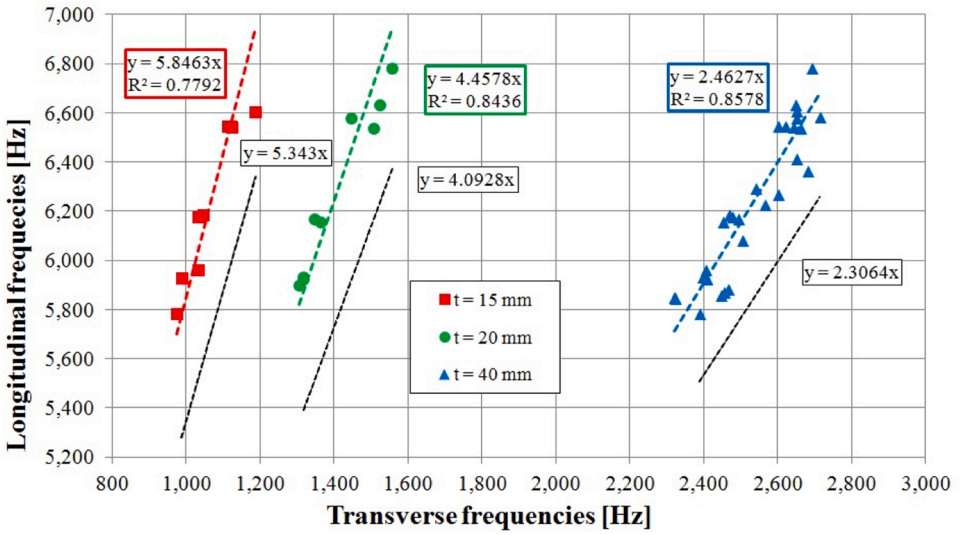

Fig. 16. Comparison between the resonant frequencies for various sample thickness.

As water vaporizes through the capillary net, the porous structure of the material becomes more evident, causing a decrease in density values and a reduction in strength and elastic moduli [78]. The use of additives that affect water content has also been linked to decreases in dynamic modulus [64]. Modeling cementitious materials is challenging due to the influence of humidity on their structure, which in turn affects their mechanical properties [78].

5.3.2. Relationship between elastic moduli and strengths

On the other hand, as strengths increase, both static and dynamic moduli also increase (Fig. 18 and 19).

Eq. (11) shows the correlation between the flexural strength ($f_{m,t}$) [MPa] and the dynamic elastic modulus E_d [MPa] (Fig. 18) as adjusted by a linear regression with a coefficient of determination of 0.69, which is considered acceptable.

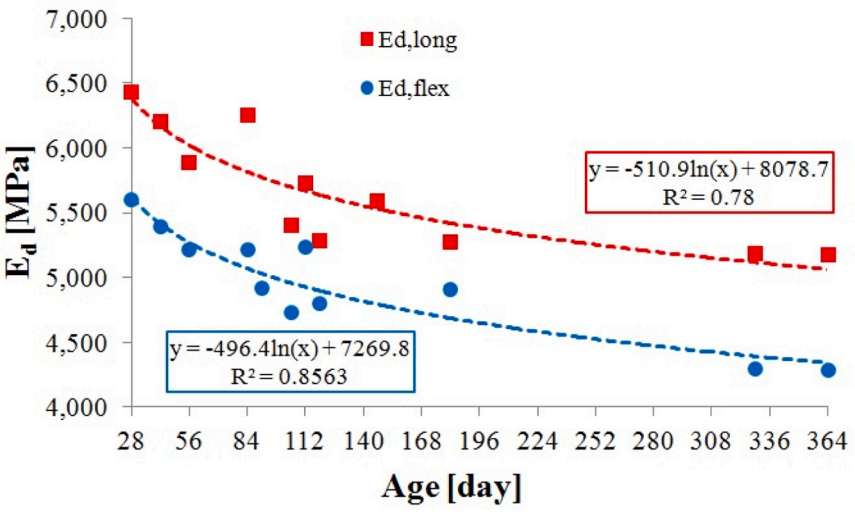

Fig. 17. Evolution of the dynamic longitudinal and transverse modulus with time.

$$E_d = 883.66 \cdot f_{m,t} + 2826.7 \tag{11}$$

Better correlations were found between the compressive strength ($f_{m,c}$) and both moduli, as shown in Fig. 19. However, the relationship between the components of the mortar is more complex than suggested by the figures, and it is restricted to each composition [79]. Various proposals exist to correlate the compressive strength with the static modulus in concrete specimens. ACI 318–19 [79] states that the square root of the modulus is proportional to the compressive strength, while Eurocode 2 [80] states that the modulus is proportional to the 0.3 square of $f_{m,c}$. When discussing Fig. 13b, other possibilities were commented. Carrasco et al. [27] suggested a linear relationship for mortars with high R^2 (0.94), while Haach et al. [7] preferred a potential law to correlate them (R^2 = 0.92). The static modulus presented in Fig. 19 is obtained from the compressive strength, which, according to Fig. 13b, shows better accuracy and is generally adopted as the static elastic modulus in the literature [25]. The introduction of gauges in the flexural test results in higher dispersion of the static modulus data. The potential relationship fits the data best, with a high R^2 (0.86). Eq. (12) proposes the relationship between compressive strength ($f_{m,c}$ in MPa) and static modulus (E_s in MPa), with an exponent of 0.75.

$$E_s = 1163.5 \cdot f_{m,c}^{3/4} \tag{12}$$

Regarding the correlations between dynamic modulus and compressive strength, better correlations are typically achieved using a power relationship ($R^2 = 0.98$ [25] and $R^2 = 0.96$ [7]) or a logarithmic equation. In the case of the latter, an R^2 value of 0.78 [27] was obtained, which increased to 0.99 when distinguishing between mortar types. For relating the dynamic modulus, E_s (MPa), and the compressive strength, $f_{m,c}$ (MPa), we propose a linear regression (Eq. 13) with high accuracy ($R^2 = 0.96$).

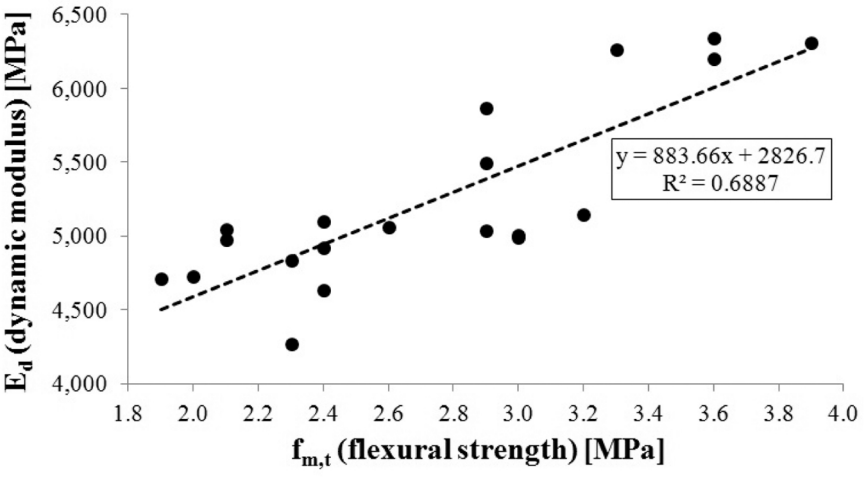

Fig. 18. Relationship between the dynamic elastic modulus and the flexural strength of the mortar.

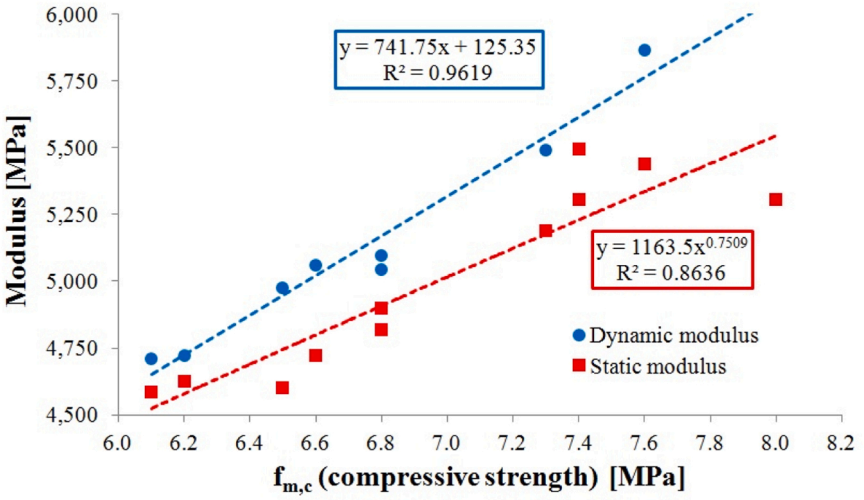

Fig. 19. Relationship between the dynamic and the static elastic modulus and the compressive strength of the mortar.

$$E_d = 741.75 \cdot f_{m,c} + 125.35 \tag{13}$$

The correlation between compressive strength and dynamic modulus is stronger than that with the static modulus. This is due to the inherent variability in the procedures involved in static tests, whereas acoustic tests show low dispersion of results [25]. Other authors have also commented this fact [7,25,27].

5.3.3. Relationship between the static and dynamic elastic moduli

Research has shown that the dynamic elastic modulus of concrete is higher than its static modulus [7,81]. Mehta and Monteiro [82] found that the dynamic elastic modulus of high-, medium-, and low-strength concretes was 20%, 30%, and 40% higher than their respective static moduli. This behavior was also observed in mortar with varying strengths, depending on the sand/cement ratios [7]. The difference between the dynamic and static moduli is influenced by factors such as sample size and shape, age, and magnitude [37]. The type of procedure selected has an impact on the results. Static tests may have misalignments in load centering, irregularities on the top and bottom faces, and gauge placement [25,42]. Literature reports differences of around 17% [7,37,42,64], with values up to 30% and 40% [25,83]. This difference occurs because the static modulus is calculated at the beginning of the stress-strain curve for a very small instantaneous strain increment.

Various equation types have been proposed to correlate mortar elastic moduli. Valentini et al. [26] identified a linear equation as

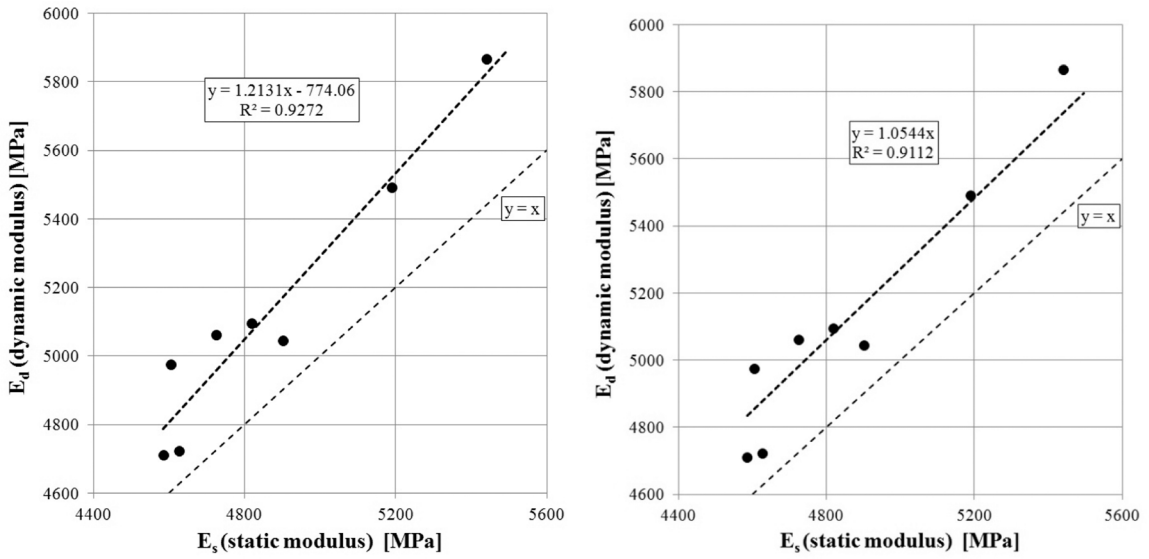

Fig. 20. Comparison between the dynamic and static elastic modulus by means of a linear regression, a) with intercept, b) without intercept.

the best fit for the data. Carrasco et al. [27] proposed a logarithmic correlation for all mortar types in their research, with an R^2 value of 0.88. The R^2 value increased to 0.99 when mortar types (granular and fine + granular) were considered separately. Haach et al. [25] proposed linear equations without intercept, with coefficients of 1.3191 and 1.318, to relate the static modulus and the dynamic modulus from the flexural and transversal modes, respectively, with an R^2 value of 0.97. This suggests that dynamic moduli are 32% higher than static ones. In a subsequent study, Haach et al. [7] proposed both a linear and a power law equation to correlate the moduli, with R^2 values of 0.94 and 0.96, respectively. The linear equation indicates that the dynamic modulus is 57% higher than the static modulus.

Fig. 20 presents a comparison between the static elastic modulus under compressive load and the dynamic modulus for the standardized sample series (MP10, MP15, MP16, MP23, MP24, and MP32). A linear regression model is proposed with an intercept (Fig. 20a) (Eq. (14)) and without an intercept (Eq. (15)) (Fig. 20b), both with similar determination coefficients. The accuracy of the models is similar to that of previous studies. In this case, the dynamic modulus is slightly higher than the static modulus by 5%, as shown in other studies [35,47]. Other researchers have exhibited greater differences between the two moduli [7,25,27].

$$E_d = 1.2131 \cdot E_s - 774.06 \tag{14}$$

$$E_d = 1.0544 \cdot E_s \tag{15}$$

5.4. Elasticity modulus of in situ samples

The dynamic modulus from longitudinal vibration mode ($E_{d,long}$) was determined to be 4890 MPa for the samples extracted from mortars placed in a real building (Table 7). For $E_{d,trans}$, a value of 4060 MPa was obtained. These values indicate a reduction of approximately 1550 MPa when compared to all the samples manufactured in the laboratory and tested at 28 days. This represents a variation of 24% and 27% compared to the values of $E_{d,long}$ and $E_{d,trans}$, respectively. Compared to the standardized samples at 28, which achieved a higher dynamic modulus, there is a reduction of 25% and 31% in $E_{d,long}$ and $E_{d,trans}$, respectively, in the field samples. The strength loss due to damages caused on the surface during the extraction and cutting of the samples is not quantified. Furthermore, the study did not take into account other factors that may contribute to strength loss, such as the surface contact of the block or the compaction procedure of the rendering mortars when applied to surfaces, different from the ones in laboratory tests. In summary, the dynamic modulus of in situ samples was found to be 25–30% lower than that of laboratory samples at 28 days.

5.5. Size effect

The strength of a structure varies depending on the randomness of the material's strength caused by its lack of homogeneity. To ensure clarity, statistical concepts should be applied to increase the probability of identifying small defects in strength as the sample size increases. According to theory, the flexural strength of non-standardized samples is expected to be higher than that of larger standardized samples. Fig. 21 displays the time evolution of the flexural strength, the only available characteristic for all thicknesses (40, 20, and 15 mm), as the compressive strength cannot be calculated in standardized samples.

It was found that reducing the thickness of the samples results in an increase in strength. Specimens with a thickness of 20 mm and 15 mm exhibit a strength increase of 18% and 25%, respectively, when compared to the standardized thickness of 40 mm, despite the known strength loss over time.

Fig. 22 presents the evolution of the dynamic Young modulus over time, calculated from the resonant frequency in the longitudinal vibration mode, for all sample thicknesses.

One conclusion that can be drawn from the numerical analysis is that the fundamental vibration frequency in the longitudinal vibration mode, used to calculate $E_{d,long}$, is approximately similar for each of the tested thicknesses. Therefore, the curves in the figure should be similar. However, there are some differences depending on the dimensions of the samples, as shown in Fig. 22. The thinner the sample, the higher the values obtained. For a thickness of 20 mm, there is a 6% increase compared to the standardized thickness of 40 mm. Similarly, for 15 mm-thick samples, the deformation modulus increases by almost 8%. Figs. 21 and 22 do not aim to present equations predicting mechanical properties as a function of age, but rather to illustrate the decreasing trend of properties for each thickness. Although the equations may not be highly accurate, they are statistically significant (with a p-value of the F-test < 0.05) and all coefficients have a 95% probability of being different from zero.

There is always a probabilistic effect on studies regarding the size effect, in the form of random variation. However, it may not be

Table 7
Mortar flexural and compressive strength at 28 days.

Sample	Age (days)	Thickness [mm]	Width [mm]	Flexural strength [MPa]	$E_{d,long}$ [MPa]	$E_{d,trans}$ [MPa]
E	~ 1000	40	15	2.4	5041	4226
E	~ 1000	15	40	2.4	5041	4218
F	~ 1000	40	15	2.3	4736	3805
F	~ 1000	15	40	2.3	4736	3980
Average of in situ specimens	~ 1000	40	15	2.35	4889	4057
Average of samples of 40 × 40 × 160 at 28 days	28	40	40	2.72	6517	5925
Average of all the samples at 28 days	28	any	40	2.94	6440	5600

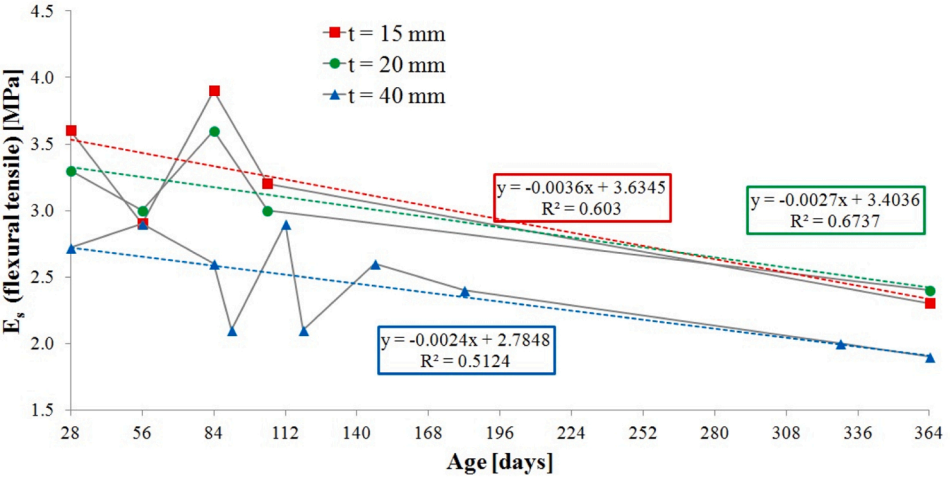

Fig. 21. Evolution of the flexural strength with time for various sample thicknesses.

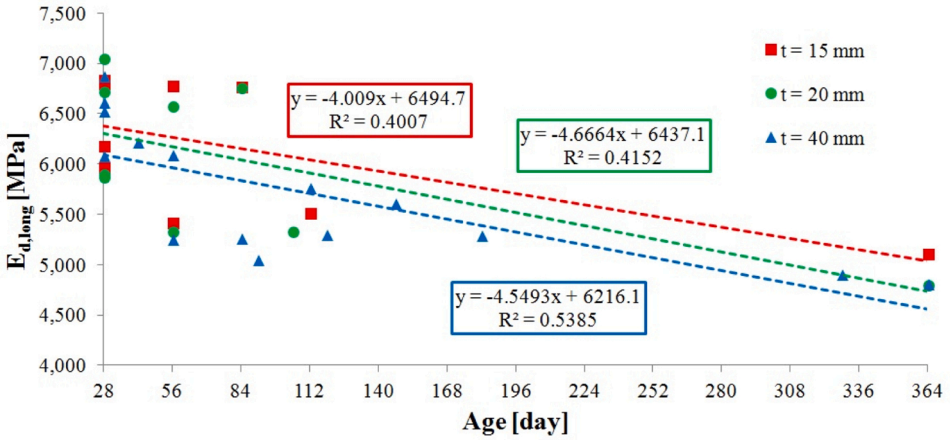

Fig. 22. Evolution of $E_{d,long}$ with time for all the sample thicknesses.

statistically significant to apply the same standardized procedures to smaller sample sizes [1]. This possibility was noted when the strain gauge on the lower face was used as reinforcement in the flexural test. In the impact vibration test, the weight of the devices can influence smaller samples due to increased density and calculated modulus.

5.6. Poisson coefficient

The procedure for determining the dynamic modulus [39] requires an estimation of the Poisson coefficient (ν) to determine the dynamic modulus in transverse vibration. Various studies have proposed different values for this constant. For concrete, a value between 1/6 and 1/3 is generally suggested [38]. For mortars, values around 0.20 are proposed, which can be calculated from static

Table 8
Calculation of Poisson coefficient.

Sample	Age (days)	Thickness (mm)	Width (mm)	Longitudinal frequency (Hz)	$E_{d,long}$ (MPa)	Torsional frequency (Hz)	G (MPa)	Poisson coefficient (ν)
PM10	182	40	40	6068	5723	3584	2374	0.21
MP24	56	40	40	5999	5468	3541	2255	0.21
PM24	84	40	40	6004	5465	3548	2258	0.21
PM32	56	40	40	6220	6025	3675	2488	0.21
PM32	112	40	40	6191	5983	3648	2458	0.22
E	1000	15	40	6144	5771	2244	2408	0.20
F	1000	15	40	5932	5276	2416	2174	0.21

tests [56] or dynamic tests [26].

Nonetheless, the procedure used to obtain it involves measuring the resonant frequency in the torsional vibration mode and calculating the shear modulus. This value, along with the dynamic Young modulus of the longitudinal vibration mode, allows for an accurate calculation of the Poisson coefficient. To achieve this, the accelerometer must be placed in the position corresponding to the torsional mode, which requires a new test. The test was not repeated for all specimens due to the expected low variation of the value on a homogeneous sample range [56]. Table 8 presents the results obtained. Two samples were tested at different ages, with each value being the average of three samples (A, B, and C). Additionally, other specimens were individually tested, namely PM10, E1, and F1. The last two were extracted from in situ mortars.

A constant value of 0.21 was obtained for all specimens. This value was then used to calculate the dynamic modulus in the transverse vibration mode, without any estimation uncertainty.

6. Conclusions

The objective of this research was to determine the dynamic elastic modulus of a rendering mortar in situ using impact vibration. A simple, accurate, and reliable technology is presented for obtaining the dynamic elastic constants from the natural vibration frequencies. The procedure proposed in the ASTM C215 standard [39] for concrete specimens can be replicated for mortars, allowing for non-destructive testing and easy repetition. Elastic constants (E, G, and ν) can be predicted in samples of various sizes.

Tests showed that for the analyzed rendering mortar, the dynamic modulus from the longitudinal vibration mode ($E_{d,long}$) was higher than that from the transverse mode ($E_{d,trans}$). However, when measures were taken with a uniaxial accelerometer, the difference was lower, with $E_{d,long} = 5401$ MPa and $E_{d,trans} = 5348$ MPa. The use of a triaxial accelerometer resulted in greater scatter. Based on the suggestion to average the dynamic modulus calculated from both vibration modes, we obtained an adjusted value of 5500 MPa for the dynamic elastic modulus of the mortar under fixed laboratory conditions. We also observed a decrease in the modulus over time. The Poisson coefficient ($\nu = 0.21$) is consistent with values reported in the literature. The dynamic modulus obtained was compared to the one obtained for the same material in a static test (EN-1352, 1997) [48] with normalized specimens of 40 × 40 × 160 mm. The results showed that both moduli evolve similarly with time and can be easily correlated with a linear regression and high accuracy.

Tests conducted on in situ specimens of the same mortar showed a reduction in the dynamic modulus of approximately 1550 MPa, which represents a decrease of 25–30% compared to specimens tested in the laboratory after 28 days.

Tests were conducted to determine the flexural and compressive strength of the mortar at different ages and thicknesses. The results showed an average flexural strength of 2.72 MPa and an average compressive strength of 7.2 MPa at 28 days. A simple linear regression with a high determination coefficient (R^2) of 0.938 was used to correlate the results. The strain-stress curve of the mortar was obtained from the flexural test. It was observed that the material exhibits a long elastic span without a plastic zone before rupture, confirming a quasi-fragile behavior. Additionally, equations were proposed to correlate the elastic moduli (both dynamic and static) with the flexural and compressive strengths. A linear regression showed a strong correlation ($R^2 = 0.96$) between the dynamic modulus and compressive strength. It is recommended to conduct a numeric simulation using a finite element analysis device before identifying the frequencies associated with each vibration mode to avoid errors during testing.

In summary, the study confirmed the feasibility of calculating the elastic dynamic modulus of a specific mortar using concrete standards. The results can be easily correlated with other mechanical properties with high accuracy. However, caution must be exercised when applying the proposed equations to other mixtures. However, other researchers can observe similarities in other mortars, which can be useful for relating mechanical parameters. Future research will include a deeper analysis of the evolution of moduli over time.

Funding

This research did not receive any specific grant from funding agencies in the public, commercial, or not-for-profit sectors.

CRediT authorship contribution statement

Perez-Acebo Heriberto: Data curation, Formal analysis, Investigation, Methodology, Software, Validation, Writing – original draft, Writing – review & editing. **Salas Miguel Ángel:** Data curation, Formal analysis, Investigation, Resources, Software, Validation, Visualization. **Aragón-Torre Ángel:** Conceptualization, Data curation, Funding acquisition, Methodology, Project administration, Resources, Software, Supervision, Validation, Visualization, Writing – original draft. **Aragón Guillermo:** Conceptualization, Data curation, Formal analysis, Investigation, Methodology, Software, Validation, Writing – review & editing.

Declaration of Competing Interest

The authors declare that they have no known competing financial interests or personal relationships that could have appeared to influence the work reported in this paper.

Data availability

Data will be made available on request.

References

[1] M. Drdácký, Non-standard testing of mechanical characteristics of historic mortars, Int. J. Archit. Herit. 5 (4-5) (2011) 383–394, https://doi.org/10.1080/15583051003717788.

[2] Steil, R.O., Calçada, L.M.L., Oliveira, A.L., Martins, V.C., Prudêncio, L.R.Jr.,2001. Influência do tipo de argamassa no fator de eficiência e na deformabilidade de alvenarias de blocos de concreto. In: Proceedings of Anais do IV simpósio Brasileiro de tecnologia de argamassas [inPortuguese].

[3] Cunha, E.H., Guimarães, G.N., Carasek, H.,2001. Influência do tipo de argamassa na resistência à compressão da alvenaria estrutural. In: Proceedings of Anais do IV simpósio Brasileiro de tecnologia dea rgamassas; [in Portuguese].

[4] P. Wiehle, M. Brinkmann, Material behaviour of unstabilised earth block masonry and its components under compression at varying relative humidity, Case Stud. Constr. Mater. 17 (2022) e01663, https://doi.org/10.1016/j.cscm.2022.e1663.

[5] G. Mohamad, P.B. Lourenço, H.R. Roman, Mechanics of hollow concrete block masonry prisms under compression: review and prospects, Cem. Concr. Compos. 29 (3) (2007), https://doi.org/10.1016/j.cemconcomp.2006.11.003.

[6] S. Deniz, S.T. Erdogan, Prediction of elastic moduli development of cement mortars using early age measurements, J. Mater. Civ. Eng. 27 (1) (2015) 04014102, https://doi.org/10.1061/(ASCE)MT.1943-5533.0001025.

[7] V.G. Haach, R. Carrazedo, M.F. Oliveira, Resonant acoustic evaluation of mechanical properties of masonry mortars, Constr. Build. Mater. 152 (2017) 494–505, https://doi.org/10.1016/j.conbuildmat.2017.07.032.

[8] H. Chu, W. Shi, Q. Wang, L. Gao, D. Wang, Feasibility of manufacturing self-compacting mortar with high elastic modulus by Al2O3 micro powder: A preliminary study, Constr. Build. Mater. 340 (2022) 127736, https://doi.org/10.1016/j.conbuildmat.2022.127736.

[9] K. Evgeny, M. Ernest, P. Valerii, M. Ilshat, I. Ruslan, A.R. De Azevedo, Experimental investigation of the deformability of the masonry vault in church historical building, Case Stud. Constr. Mater. 18 (2023) e01833, https://doi.org/10.1016/j.cscm.2023.e01833.

[10] J.F. Lizárraga, J.J. Pérez-Gavilán, Parameter estimation for nonlinear analysis of multi-perforated concrete masonry walls, Constr. Build. Mater. 141 (2017) 353–365, https://doi.org/10.1016/j.conbuildmat.2017.03.008.

[11] G. Aragon, A. Aragon, A. Santamaria, A. Esteban, F. Fiol, Physical and mechanical characterization of a commercial rendering mortar using destructive and non-destructive techniques, Constr. Build. Mater. 224 (2019) 835–849, https://doi.org/10.1016/j.conbuildmat.2019.07.034.

[12] I. Perez, M. Toledano, J. Gallego, J. Taibo, Mechanical properties of hot mix asphalt made with recycled aggregates from reclaimed construction and demolition debris, Mater. De. Constr. 57 (285) (2007) 17–29, https://doi.org/10.3989/mc.2007.v57.i285.36.

[13] M.A. Salas, H. Pérez-Acebo, Introduction of recycled polyurethane foam in mastic asphalt. Gradevinar 70 (5) (2018) 403–412, https://doi.org/10.14256/JCE.2181.2017.

[14] H. Gonzalo-Orden, A. Linares-Unamunzaga, H. Perez-Acebo, J. Díaz-Minguela, Advances in the study of bhe behavior of Full-Depth Reclamation (FDR) with cement, Appl. Sci. 9 (15) (2019) 3055, https://doi.org/10.3390/app9153055.

[15] S.A. Zamora-Castro, R. Salgado-Estrada, L.C. Sandoval-Herazo, R.A. Melendez-Armenta, E. Manzano-Huerta, E. Yelmi-Carrillo, A.L. Herrera-May, Sustainable development of concrete through aggregates and innovative materials: a review, Appl. Sci. 11 (2) (2021) 629, https://doi.org/10.3390/app11020629.

[16] V. Arularasi, T. Pachiappan, S. Avudaiappan, S.N. Raman, P. Guindos, M. Amran, R. Fediuk, N.I. Vatin, Effects of admixtures on energy consumption in the process of ready-mixed concrete mixing, Materials 15 (12) (2022) 4143, https://doi.org/10.3390/ma15124143.

[17] H. Gharibi, D. Mostofinejad, Thermal and mechanical properties of concrete containing porcelain ceramic tile waste as fine and coarse aggregates, Mag. Concr. Res. (2022) 1–12, https://doi.org/10.1680/jmacr.22.00076.

[18] Y. Aocharoen, P. Chotickai, Compressive mechanical properties of cement mortar containing recycled high-density polyethylene aggregates: stress–strain relationship, Case Stud. Constr. Mater. 15 (2021) e00752, https://doi.org/10.1016/j.cscm.2021.e00752.

[19] J.Q. Wang, Mechanics performance of cement mortar modified by carboxylic styrene butadiene latex, Adv. Mater. Res. 908 (2014) 141–144, https://doi.org/10.4028/www.scientific.net/AMR.908.141.

[20] M.A. Salas, H. Perez-Acebo, V. Calderón, H. Gonzalo-Orden, Analysis and economic evaluation of the use of recycled polyamide powder in masonry mortars, Polymers 12 (11) (2020) 2657, https://doi.org/10.3390/polym12112657.

[21] M. EL Boukhari, O. Merroun, C. Maalouf, F. Bogard, B. Kissi, Mechanical performance of cement mortar with olive pomace aggregates and olive mill wastewater: an experimental investigation, Cogent Eng. 10 (1) (2023) 2212522, https://doi.org/10.1080/23311916.2023.2212522.

[22] I.Y. Hakeem, R.O. Abd-Al Ftah, B.A. Tayeh, R.D.A. Hafez, Eggshell as a fine aggregate replacer with silica fume and fly ash addition in concrete: a sustainable approach, Case Stud. Constr. Mater. 18 (2023) e01842 https://doi.org/j.cscm.2023.e01842.

[23] Q. Wang, H. Chu, W. Shi, J. Jiang, F. Wang, Feasibility of preparing self-compacting mortar via municipal solid waste incineration bottom ash: an experimental study, Arch. Civ. Mech. Eng. 23 (4) (2023) 251, https://doi.org/10.1007/s43452-023-00794-5.

[24] H. Li, H. Chu, Q. Wang, J. Tang, Feasibility of producing eco-friendly self-compacting mortar with municipal solid waste incineration bottom ash: a preliminary study, Case Stud. Constr. Mater. 19 (2023) e02309, https://doi.org/10.1016/j.cscm.2023.e02309.

[25] V.G. Haach, R. Carrazedo, L.M.F. Oliveira, M.R.S. Corrêa, Application of acoustic tests to mechanical characterization of masonry mortars, NDTE Int. 59 (2013) 18–24, https://doi.org/10.1016/j.ndteint.2013.04.013.

[26] L. Valentini, M. Parisatto, V. Russo, G. Ferrari, J.W. Bullard, R.J. Angel, M.C. Dalconi, G. Artioli, Simulation of the hydration kinetics and elastic moduli of cement mortars by microstructural modelling, Cem. Concr. Compos. 52 (2014) 54–63, https://doi.org/10.1016/j.cemconcomp.2014.05.005.

[27] E.V.M. Carrasco, M.D.C. Magalhaes, W.J.D. Santos, R.C. Alves, J.N.R. Mantilla, Characterization of mortars with iron ore tailings using destructive and non destructive tests, Constr. Build. Mater. 131 (2017) 31–38, https://doi.org/10.1016/j.conbuildmat.2016.11.065.

[28] A. Su, T. Chen, X. Gao, Q. Li, L. Qin, Effect of carbonation curing on durability of cement mortar incorporating carbonated fly ash subjected to Freeze-Thaw and sulfate attack, Constr. Build. Mater. 341 (2022) 127920, https://doi.org/10.1016/j.conbuildmat.2022.127920.

[29] X.T. Yu, D. Chen, J.R. Feng, Y. Zhang, Y.D. Liao, Behavior of mortar exposed to different exposure conditions of sulfate attack, Ocean Eng. 157 (2018) 1–12, https://doi.org/10.1016/j.oceaneng.2018.03.017.

[30] A.I. Marques, J. Morais, C. Santos, P. Morais, M. do Rosário Veiga, Static elasticity modulus analysis of coating mortars, Procedia Struct. Integr. 17 (2019) 1002–1009, https://doi.org/10.1016/j.prostr.2019.09.001.

[31] X. Jin, Z. Li, Dynamic property determination for early-age concrete, Acids Mater. J. 98 (5) (2001) 365–370, https://doi.org/10.14359/10725.

[32] V. Giner, S. Ivorra, F. Baeza, E. Zornoza, B. Ferrer, Silica fume admixture effect on the dynamic propertes of concrete. Constr. Build. Mater. 25 (8) (2011) 3272–3277, https://doi.org/10.1016/j.conbuildmat.2011.03.014.

[33] X. Lu, Q. Sun, W. Feng, J. Tian, Evaluation of dynamic modulus of elasticity of concrete using impact-echo method, Constr. Build. Mater. vol. 47 (2013) 231–239, https://www.doi.org/10.10167j.conbuildmat.2013.04.043.

[34] J. He, D. Lei, W. Xu, In-situ measurement of nominal compressive elastic modulus of interfacial transition zone in concrete by SEM-DIC coupled method, Cem. Concr. Compos. 114 (2020) 103779, https://doi.org/10.1016/j.cemconcomp.2020.103779.

[35] A.I. Marques, J. Morais, P. Morais, M. do Rosário Veiga, C. Santos, P. Candeias, J.G. Ferreira, Modulus of elasticity of mortars: static and dynamic analyses, Constr. Build. Mater. 232 (2020) 117216, https://doi.org/10.1016/j.conbuildmat.2019.117216.

[36] International Organization for Standardization (ISO), 1982. ISO 6784:1982. Concrete – Determination of static modulus of elasticity in compression, International Organization fo Standardization.

[37] Popovics, Jonh S., Zemajtis, J., Shkolnik, I.,2008. A study of static and dynamic modulus of elasticity of concrete. ACI-CRD Final Report.

[38] Picket, G., 1945. Equations for Computing Elastic Constants from Flexural and Torsional Resonant Frequencies of Vibration of Prisms and Cylinders. Proceedings of the American Society for Testing and Materials. Portland Cement Association, 45, pp. 846–865.

[39] ASTM, ASTM-C215 (2008). Standard Test Method for Fundamental Transverse, Longitudinal, and Torsional Frequencies of Concrete Specimens, American Society for Testing and Materials, 2008.

[40] S.V. Kolluru, J.S. Popovics, S.P. Shah, Determining elastic properties of concrete using vibrational resonance frequencies of standard test cylinders, Cem. Concr. Aggreg. 22 (2000) 81–89.
[41] Malaikah, A., Al-Saif, K., Al-Zaid, R.,2004. Prediction of the dynamic modulus of elasticity of concrete under different loading conditions. International Conference on Concrete Engineering and Technology, 2004.
[42] J.R. Rosell, I.R. Cantalapiedra, Simple method of dynamic Young's modulus determination in lime and cement mortars, Mater. De. Construccion 61 (2011) 39–48, https://doi.org/10.3989/mc.2010.53509.
[43] W. Martínez-Molina, A.A. Torres-Acosta, J.C. Jáuregui, H.L. Chávez-García, E.M. Alonso-Guzmán, M. Graff, J.C. Arteaga-Arcos, Predicting concrete compressive strength and modulus of rupture using different NDT techniques, Adv. Mater. Sci. Eng. 2014 (2014) 742129, https://doi.org/10.1155/2014/742129.
[44] T. Matusinović, S. Kurajica, J. Šipušić, The correlation between compressive strength and ultrasonic parameters of calcium aluminate cement materials, Cem. Concr. Res. 34 (8) (2004) 1451–1457, https://doi.org/10.1016/j.cemconres.2004.01.024.
[45] T. Voigt, Z. Sun, S.P. Shah, Comparison of ultrasonic wave reflection method and maturity method in evaluating early-age compressive strength of mortar, Cem. Concr. Compos. 28 (4) (2006) 307–316, https://doi.org/10.1016/j.cemconcomp.2006.02.003.
[46] S.H. Han, J.K. Kim, Effect of temperature and age on the relationship between dynamic and static elastic modulus of concrete, Cem. Concr. Res. 34 (7) (2004) 1219–1227, https://doi.org/10.1016/j.cemconres.2003.12.011.
[47] Cikrle, P., Adámek, J., Stehlik, M.,2018. Ultrasonic testing of properties of mortars. In Structural Analysis of Historical Constructions-2 Volume Set: Possibilities of Numerical and Experimental Techniques-Proceedings of the IVth Int. Seminar on Structural Analysis of Historical Constructions, 10–13 November 2004, Padova, Italy (p. 407). CRC Press.
[48] CEN, 1997. UNE EN 1352:1997. Determination of static modulus of elasticity under compression of autoclaved aerated concrete or lightweight aggregate concrete with open structure. Comité Européen de Normalisation/European Commission for standardization, Brussels, Belgium.
[49] J. Schulze, Influence of water-cement ratio and cement content on the properties of polymer-modified mortars, Cem. Concr. Res. 29 (6) (1999) 909–915, https://doi.org/10.1016/S0008-8846(99)00060-5.
[50] H. Paiva, L.P. Esteves, P.B. Cachim, V.M. Ferreira, Rheology and hardened properties of single-coat render mortars with different types of water retaining agents, Constr. Build. Mater. 23 (2) (2009) 1141–1146, https://doi.org/10.1016/j.conbuildmat.2008.06.001.
[51] CEN, EN 998:2010. Specification for Mortar for Masonry, Comité Européen de Normalisation/European Commission for standardization, Brussels, Belgium, 2010.
[52] CEN, EN 998-1:2010. Specification for Mortar for Masonry – Part 1: Rendering and Plastering Mortar, Comité Européen de Normalisation/European Commission for standardization, Brussels, Belgium, 2010.
[53] BSI, 1992. BS 5628–1, Code of Practice for Use of Masonry: Part 1: Structural Use of Unreinforced Masonry. (1992). British Standard. doi: 10.3403/BS5628.
[54] CEN, EN 196-1:2005 Methods of testing cement – Part 1: Determination of strength, Comité Européen de Normalisation/European Commission for standardization, Brussels, Belgium, 2005.
[55] CEN, EN 1015-11:1999. Methods of Test for Mortar for Masonary - Part 11: Determination of Flexural and Compressive Strength of Hardened Mortar, Comité Européen de Normalisation/European Commission for standardization, Brussels, Belgium, 1999.
[56] I.O. Toma, D. Covatariu, A.M. Toma, G. Taranu, M. Budescu, Strength and elastic properties of mortars with various percentages of environmentally sustainable mineral binder, Constr. Build. Mater. 43 (2013) 348–361, https://doi.org/10.1016/j.conbuildmat.2013.02.061.
[57] A. Nagy, Determination of E-modulus of young concrete with nondestructive method, J. Mater. Civ. Eng. 9 (1) (1997) 15–20.
[58] CEN, EN 14146:2004. Natural Stone Test Methods – Determination of the Dynamic Modulus of Elasticity (by Measuring the Fundamental Resonance Frequency, Comité Européen de Normalisation/European Commission for standardization, Brussels, Belgium, 2004.
[59] CEN, EN ISO 12680-1: 2007. Methods of Test for Refractory Products – Part 1: Determination of Dynamic Young's Moduls (Moe) by Impulse Excitation of Vibration (Iso 12680-1:2005), Comité Européen de Normalisation/European Commission for standardization, Brussels, Belgium, 2007.
[60] R. Jones, The non-destructive testing of concrete, Mag. Concr. Res. 1 (2) (1949) 67–78, https://doi.org/10.1680/macr.1949.1.2.67.
[61] V. Revilla-Cuesta, J.Y. Shi, M. Skaf, V. Ortega-López, J.M. Manso, Non-destructive density-corrected estimation of the elastic modulus of slag-cement self-compacting concrete containing recycled aggregate, Dev. Built Environ. 12 (2022) 100097, https://doi.org/10.1016/j.dibe.2022.100097.
[62] CEN, EN 1015-2:1999. Methods of Test for Mortar for Masonary - Part 2: Bulk Sampling of Mortars and Preparation of Test Mortars, Comité Européen de Normalisation/European Commission for standardization, Brussels, Belgium, 1999.
[63] V.G. Haach, G. Vasconcelos, P.B. Lourenço, Influence of aggregates grading and water/cement ratio in workability and hardened properties of mortars, Constr. Build. Mater. 25 (6) (2011) 2980–2987, https://doi.org/10.1016/j.conbuildmat.2010.11.011.
[64] N. Swamy, G. Rigby, Dynamic properties of hardened paste, mortar and concrete, Matér. Et. Constr. 4 (1) (1971) 13–40, https://doi.org/10.1007/BF02473927.
[65] Esteves, L.P., Cachim, P., Ferreira, V.M.,2007. Mechanical properties of cement mortars with superabsorbent polymers. In: Advances in Construction Materials, Springer, Berlin, 451–462, https://www.doi.org/10.1007/978-3-540-72448-3_45.
[66] H. Wang, M. Jiang, M. Hang, G. Zhou, M. Sun, X. Liu, Research on the mechanical properties and frost resistance of aeolian sand 3D printed mortar, Case Stud. Constr. Mater. 19 (2023) e02332, https://doi.org/10.1016/j.cscm.2023.e02332.
[67] M.S. Nasr, A. Shubbar, T.M. Hashim, A.A. Abadel, Properties of a low-carbon binder-based mortar made with waste LCD glass and waste rope (Nylon) fibers, Processes 11 (5) (2023) 1533, https://doi.org/10.3390/pr11051533.
[68] G.D.M.S. Gidrão, R. Carrazedo, R.M. Bosse, L. Silvestro, R. Ribeiro, C.F.P. de Souza, Numerical modeling of the dynamic elastic modulus of concrete, Materials 16 (11) (2023) 3955, https://doi.org/10.3390/ma16113955.
[69] E.T. Dawood, A.S. Shawkat, M.H. Abdullah, Flexural performance of ferrocement based on sustainable high-performance mortar, Case Stud. Constr. Mater. 15 (2021) e00566.
[70] X. Chen, S. Wu, J. Zhou, Influence of porosity on compressive and tensile strength of cement mortar, Constr. Build. Mater. 40 (2013) 869–874, https://doi.org/10.1016/j.conbuildmat.2012.11.072.
[71] I. Yurtdas, H. Peng, N. Burlion, F. Skoczylas, Influences of water by cement ratio on mechanical properties of mortars submitted to drying, Cem. Concr. Res. 36 (7) (2006) 1286–1293, https://doi.org/10.1016/j.cemconres.2005.12.015.
[72] H. Paiva, L.P. Esteves, P.B. Cachim, V.M. Ferreira, Rheology and hardened properties of single-coat render mortars with different types of water retaining agents, Constr. Build. Mater. 23 (2) (2009) 1141–1146, https://doi.org/10.1016/j.conbuildmat.2008.06.001.
[73] British Standard, 1992. BS 5628–1:1992. Code of practice for use of masonry. Part 1: Structural use of unreinforced masonry.
[74] X. Lu, Q. Sun, W. Feng, J. Tian, Evaluation of dynamic modulus of elasticity of concrete using impact-echo method, Constr. Build. Mater. 47 (2013) 231–239, https://doi.org/10.1016/j.conbuildmat.2013.04.043.
[75] L.-X. Xiong, L.-J. Yu, Mechanical properties of cement mortar in sodium sulfate and sodium chloride solutions, J. Cent. South Univ. 22 (2015) 1096–1103, https://doi.org/10.1007/s11771-015-2621-8.
[76] J.N. Eiras, J.S. Popovics, M.V. Borrachero, J. Monzó, J. Payá, The effects of moisture and micro-structural modifications in drying mortars on vibration-based NDT methods, Constr. Build. Mater. 94 (2015) 565–571, https://doi.org/10.1016/j.conbuildmat.2015.07.078.
[77] P. Grassl, H.S. Wong, N.R. Buenfeld, Influence of aggregate size and volume fraction on shrinkage induced micro-cracking of concrete and mortar, Cem. Concr. Res. 40 (1) (2010) 85–93, https://doi.org/10.1016/j.cemconres.2009.09.012.
[78] I.O. Yaman, N. Hearn, H.M. Aktan, Active and non-active porosity in concrete. Part I: Experimental evidence. Mater. Struct. /Mater. Et. Constr. 34 (246 (2002) 102–109, https://doi.org/10.1007/BF02482109.
[79] ACI Committee, 318, Building Code Requirements for Structural Concrete (ACI 318-19) and Commentary, American Concrete Institute, Parmington Hills, MI, USA, 2019.
[80] CEN, 2004. EN 1992–1-1, Eurocode 2: Design of Concrete Structures – Part 1–1: General Rules and Rules for Buidling. Brussels, Belgium.
[81] W. Goldsmith, M. Polivka, T. Yang, Dynamic behavior of concrete, Exp. Mech. 6 (2) (1966) 65–79, https://doi.org/10.1007/BF02326224.
[82] P.K. Mehta, P.J. Monteiro. Concrete: Microstructure, Properties, and Materials, 3rd edition.,, McGraw-Hill, New York, 2016.